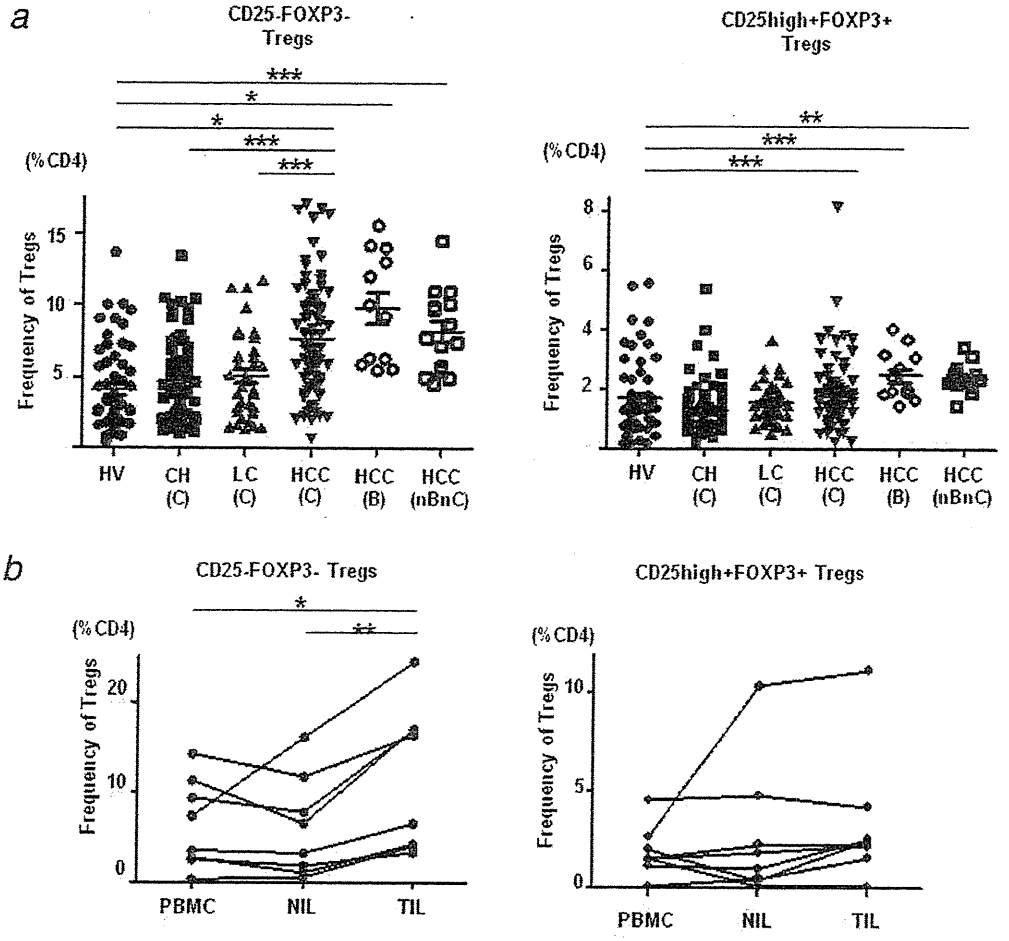

Figure 3. $CD25^{-}FOXP3^{-}$ Tregs and $CD25^{high+}FOXP3^{+}$ Tregs increase in HCC patients both in the periphery and in the liver. (*a*) The frequencies of $CD25^{-}FOXP3^{-}$ Tregs ($CD4^{+}CD25^{-}CD127^{-}$ $FOXP3^{-}$) and $CD25^{high+}FOXP3^{+}$ Tregs ($CD4^{+}CD25^{high+}CD127^{-}FOXP3^{+}$) in $CD4^{+}$ T cells were compared among the groups. HV, healthy volunteers; CH(C), LC(C), HCC (C), HCV-infected chronic hepatitis, liver cirrhosis or hepatocellular carcinoma, respectively; HCC (B), HBV-positive; HCC (nBnC), HCV-negative and HBV-negative HCC patients. The horizontal bars indicate mean ± standard deviation. *: $p < 0.05$; **: $p < 0.01$; ***: $p < 0.001$ by Kruskal–Wallis test with Dunn's multiple comparison test. (*b*) $CD25^{-}FOXP3^{-}$ Tregs and $CD25^{high+}FOXP3^{+}$ Tregs are present in tumor-infiltrating lymphocytes of HCC patients. Lymphocytes from HCC, nontumor liver tissue and PBMC were collected from identical nine HCC patients, and the frequency of $CD25^{-}FOXP3^{-}$ Tregs and $CD25^{high+}FOXP3^{+}$ Tregs in them was compared. PBMC, peripheral blood mononuclear cells; NIL, nontumor tissue infiltrating lymphocytes; TIL, tumor-infiltrating lymphocytes. *: $p < 0.05$; **: $p < 0.01$, by Friedman test with Bonferroni multiple comparison test.

IL-T4 is expressed on DC and transmits inhibitory signals after ligation with HLA-G. To confirm that the HLA-G and PD-L1 expressed in HCC are responsible for $IL10^{+}$ $CD25^{-}FOXP3^{-}$ T cell induction, we knocked down HLA-G and/or PD-L1 in Huh7 cells by siRNA and subjected them to the abovementioned *in vitro* cultures (Fig. 5*d*). As a result, $IL10^{+}$ $CD25^{-}FOXP3^{-}$ T cell frequency is significantly decreased in the presence of siRNA-treated HCC, but not with mock-transfected HCC (Fig. 5*e*). These results demonstrate that DC and HCC cells are actively involved in IL-10^{+} $CD25^{-}FOXP3^{-}$ T cell induction, in which PD-L1, IL-T4 and HLA-G are indispensible.

Discussion

In this study, we focused on $CD25^{-}FOXP3^{-}$ Tregs in HCC patients, which are distinct from $CD25^{high+}FOXP3^{+}$ natural Tregs in cellular phenotypes, genetic profiles and functional aspects. We demonstrated that; (*i*) $CD4^{+}CD127^{-}CD25^{-}$ cells (as defined as $CD25^{-}FOXP3^{-}$ cells in this study) are endowed with suppressive capacity comparably with

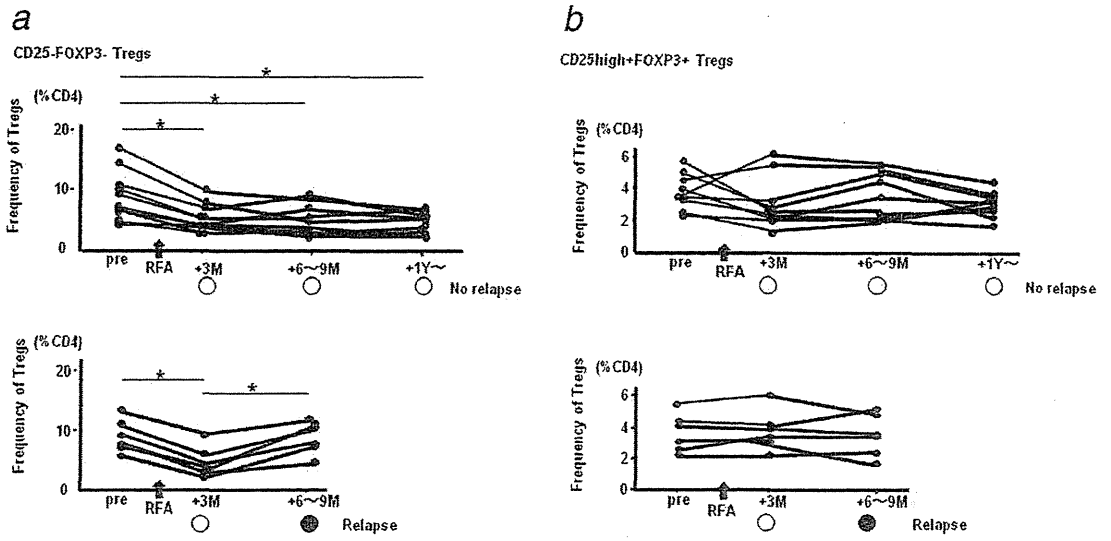

Figure 4. $CD25^{-}FOXP3^{-}$ Tregs increase in parallel with post therapeutic HCC recurrence. In HCC patients who underwent RFA therapy, frequencies of $CD25^{-}FOXP3^{-}$ Tregs (*a*) and $CD25^{high+}FOXP3^{+}$ Tregs (*b*) in $CD4^{+}$ T cells are examined serially before RFA sessions and after confirmation of complete ablation of relevant HCC lesions. Open circles (○)depict the time points without HCC recurrence under CT/MRI examinations and closed circles (●)are those with detectable HCC recurrence, respectively. Arrows indicate the time points of RFA sessions. *: $p < 0.05$ by Friedman test with Bonferroni multiple comparison test.

Tumor Immunology

$CD4^{+}CD127^{-}CD25^{high+}$ cells ($CD25^{high+}FOXP3^{+}$ cells) and (*ii*) the frequency of $CD25^{-}FOXP3^{-}$ Tregs changes more dynamically than those of $CD25^{high+}FOXP3^{+}$ Tregs in correlation with post-therapeutic HCC recurrence.

Extensive studies have been carried out on the role of natural Tregs in cancer patients, of which are conventionally defined as $CD25^{high+}FOXP3^{+}$ T cells. Pharmaceutical deprivation of $CD25^{+}$ T cells *in vivo* were tried to improve immune reactivity against cancers; however, most of the study results were unsatisfactory.[19,20] Such experiences raise the possibility that the involvement of $CD25^{-}$ Tregs in the pathogenesis of certain cancers. In support for this, the existence of $CD25^{-}FOXP3^{-}$ Tregs has been reported in mice and human, in relation to viral infection or cancers.[21–23] The comparative roles of $CD25^{high+}FOXP3^{+}$ natural Tregs and $CD25^{-}$ Tregs in human diseases are still largely unknown. It is reported that CD127 expression is inversely correlated with a FOXP3 and CD127 negative population broadly encompassing regulatory cells.[11,12] Several investigators reported that CD127 expression on T cells is aberrantly regulated with regard to their functional relevance.[24,25] Taking these findings into consideration, we aimed to identify distinct type of Tregs in $CD4^{+}CD127^{-}$ population. Consequently, we found a functional regulatory subset in $CD4^{+}CD25^{-}CD127^{-}$ T cells, which differ from $CD4^{+}CD25^{high+}CD127^{-}$ Tregs in molecular profiles and inhibitory mechanisms. The profile of $CD4^{+}CD25^{-}CD127^{-}$ T cells is quite unique; they express more LAG-3, IL-21, c-Maf and PD-1 but less FOXP3, CTLA-4 and GITR than $CD4^{+}CD25^{high+}CD127^{-}$ Tregs do. In support of our results, Pot *et al.* reported that IL-27 induces IL-21 and c-Maf, which are critically involved in the differentiation of IL-10-producing Tr1.[26] As for functional aspects, we showed that $CD4^{+}CD25^{-}CD127^{-}$ cells use IL-10 as suppressive machineries, not completely but in part. Based on these characteristics, it is likely that $CD4^{+}CD25^{-}CD127^{-}FOXP3^{-}$ cells, as defined as $CD25^{-}FOXP3^{-}$ Tregs in this study, are presumed to be aforementioned Tr1 cells. Such phenotype of T cells are compatible with Tr1-like cells in human, as reported by Haringer *et al.*[14] To confirm that, several additional examinations, such as antigen-specific suppressive capacity, need to be carried out. Using tetanus toxoid as a representative of general recall antigens in this study, $CD4^{+}CD25^{-}CD127^{-}$ cells and $CD4^{+}CD25high^{+}CD127^{-}$ cells tended to be suppressive on autologous $CD4^{+}$ T cell proliferation (Supporting Information Fig. 2). Further analysis needs to be performed on this issue, using other sets of recall antigens.

To therapeutically control Tregs *in vivo*, extensive studies have been carried out to disclose the mechanisms of the induction or attraction of $FOXP3^{+}$ Tregs.[27,28] Likewise, it is tempting to consider that $CD25^{-}FOXP3^{-}$ Tregs depletion would have a favorable impact on the clinical features of the patients. Thus, identifying the molecules involved in $CD25^{-}FOXP3^{-}$, Treg induction should be carried out for the future development of Treg-oriented therapeutic approach. For this purpose, we successfully expanded $CD4^{+}CD25^{-}CD127^{-}FOXP3^{-}IL10^{+}$ cells from naive $CD4^{+}CD25^{-}$T cells. Such cultured cells contained approximately 10% of $IL\text{-}10^{+}$ cells, which subsequently

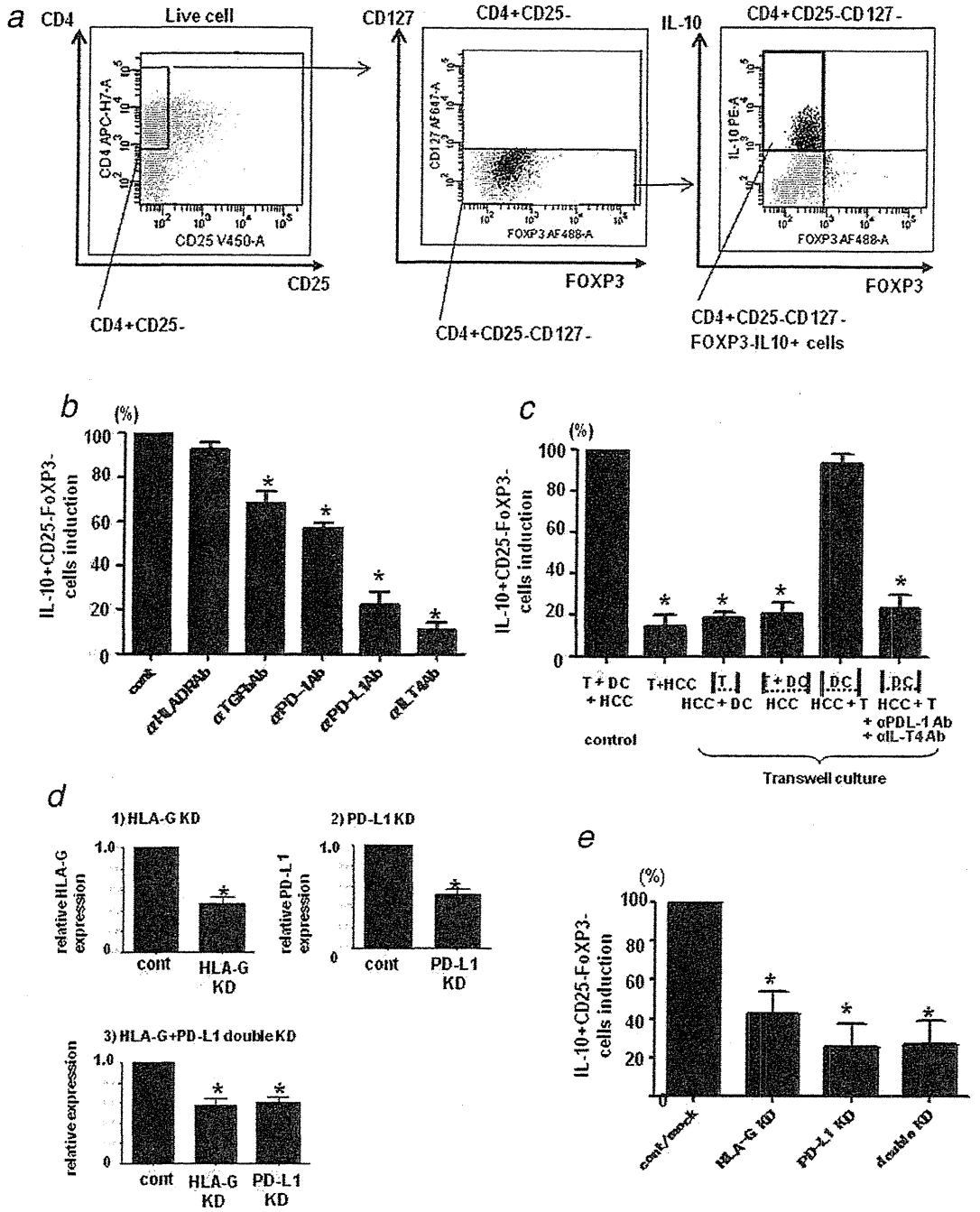

Figure 5. HLA-G and PD-L1 in HCC and IL-T4 in DC are involved in the induction of IL-10$^+$CD25$^-$FOXP3$^-$ Tregs. After culture of CD4$^+$CD45RA$^+$ naive T cells with autologous monocyte-derived dendritic cells and Huh-7 or HepG2, CD4$^+$ CD127$^-$ CD25$^-$FOXP3$^-$IL-10$^+$ T cells (IL-10$^+$CD25$^-$FOXP3$^-$ Tregs) were generated. (*a*) Representative dot plots from results of seven healthy volunteers are shown. In the abovementioned coculture system, various neutralizing/masking Abs (*b*) or transwell inserts (*c*) were added and the results were compared with the frequencies of IL-10$^+$CD25$^-$FOXP3$^-$ Tregs with or without treatments. In addition, we transfected siRNA against HLA-G and/or PD-L1 to Huh-7 and cocultured them with naive CD4$^+$ T cells and DC as the same as above. The efficiency of gene silencing was evaluated by the comparison of transcripts of HLA-G or PD-L1 with or without siRNA transfection (*d*). The frequency of IL-10$^+$CD25$^-$FOXP3$^-$ Tregs after the culture was compared with mock-transfected ones (*e*). In Figures 5-B, 5-C and 5-E, the bars indicate the ratio of IL-10$^+$CD25$^-$FOXP3$^-$ Tregs frequency (mean + standard deviation) between those with treatment and without from three series of experiments. *: $p < 0.05$ by Wilcoxon rank sum test.

tended to inhibit proliferation of allogeneic $CD4^+$ T cells (data not shown). Using this culture, we demonstrated that DCs are indispensible for IL-10^+ $CD25^-FOXP3^-$ Tregs induction *in vitro* by way of PD-1/PD-L1 and IL-T4/HLA-G pathways. Several reports showed that such molecular interactions are involved in the generation of regulatory cells in cancer patients.[29,30] In patients with HCC, a positive correlation is observed between the expression of PD-L1 or HLA-G in cancer tissue and the poorer prognosis of the patients,[31,32] suggesting that such molecules are involved in cancer development. As for HLA-G in this study, direct cellular contact between DC and HCC is not necessary in IL-10^+ $CD25^-FOXP3^-$ Tregs induction, suggesting that soluble HLA-G released from HCC may play an active role. In our hands, soluble HLA-G was measurable in culture supernatants of HCC cell lines and in serum samples from HCC patients (data not shown). Further investigation is arguably needed to elucidate whether soluble HLA-G is functional or not in HCC patients.

In summary, we demonstrate that $CD25^-FOXP3^-$ Tregs are increased in HCC patients, which change dynamically in response to HCC occurrence and post-therapeutic recurrence. Cross-talks among HCC cells, DC and $CD4^+$ T cells are required for IL-10^+ $CD25^-FOXP3^-$ Tregs induction, in which PD-L1, HLA-G and IL-T4 are critically involved. Although further investigation is needed to prove that deprivation or inactivation of $CD25^-FOXP3^-$ Tregs improves immune responses *in vivo*, such molecules could serve as targets of Treg-oriented therapeutic intervention for HCC.

Acknowledgements

The authors thank T Daimon, Department of Mathematics, Hyogo Medical University, for help with the statistical analysis; M. Hirose, Y. Kuronaka and H. Shimizu of the BD Laboratory for their technical assistance.

References

1. Parkin DM, Bray F, Ferlay J, Pisani P. Estimating the world cancer burden: globocan 2000. *Int J Cancer* 2001;94:153–6.
2. Bruix J, Sherman M. Management of hepatocellular carcinoma. *Hepatology* 2005;42: 1208–36.
3. Davila JA, Morgan RO, Shaib Y, McGlynn KA, El-Serag HB. Hepatitis C infection and the increasing incidence of hepatocellular carcinoma: a population-based study. *Gastroenterology* 2004; 127:1372–80.
4. Sakaguchi S, Yamaguchi T, Nomura T, Ono M. Regulatory T cells and immune tolerance. *Cell* 2008;133:775–87.
5. Jonuleit H, Schmitt E. The regulatory T cell family: distinct subsets and their interrelations. *J Immunol* 2003;171:6323–7.
6. Liyanage UK, Moore TT, Joo HG, Tanaka Y, Herrmann V, Doherty G, Drebin JA, Strasberg SM, Eberlein TJ, Goedegebuure PS, Linehan DC. Prevalence of regulatory T cells is increased in peripheral blood and tumor microenvironment of patients with pancreas or breast adenocarcinoma. *J Immunol* 2002;169:2756–61.
7. Ormandy LA, Hillemann T, Wedemeyer H, Manns MP, Greten TF, Korangy F. Increased populations of regulatory T cells in peripheral blood of patients with hepatocellular carcinoma. *Cancer Res* 2005;65:2457–64.
8. Fu J, Xu D, Liu Z, Shi M, Zhao P, Fu B, Zhang Z, Yang H, Zhang H, Zhou C, Yao J, Jin L, et al. Increased regulatory T cells correlate with CD8 T-cell impairment and poor survival in hepatocellular carcinoma patients. *Gastroenterology* 2007;132:2328–39.
9. Hori S, Nomura T, Sakaguchi S. Control of regulatory T cell development by the transcription factor Foxp3. *Science* 2003;299: 1057–61.
10. Ziegler SF. FOXP3: of mice and men. *Annu Rev Immunol* 2006;24:209–26.
11. Liu W, Putnam AL, Xu-Yu Z, Szot GL, Lee MR, Zhu S, Gottlieb PA, Kapranov P, Gingeras TR, Fazekas de St Groth B, Clayberger C, Soper DM, et al. CD127 expression inversely correlates with FoxP3 and suppressive function of human CD4+ T reg cells. *J Exp Med* 2006;203:1701–11.
12. Seddiki N, Santner-Nanan B, Martinson J, Zaunders J, Sasson S, Landay A, Solomon M, Selby W, Alexander SI, Nanan R, Kelleher A, Fazekas de St Groth B. Expression of interleukin (IL)-2 and IL-7 receptors discriminates between human regulatory and activated T cells. *J Exp Med* 2006;203:1693–700.
13. Hartigan-O'Connor DJ, Poon C, Sinclair E, McCune JM. Human CD4+ regulatory T cells express lower levels of the IL-7 receptor alpha chain (CD127), allowing consistent identification and sorting of live cells. *J Immunol Methods* 2007;319:41–52.
14. Haringer B, Lozza L, Steckel B, Geginat J. Identification and characterization of IL-10/IFN-gamma-producing effector-like T cells with regulatory function in human blood. *J Exp Med* 2009;206:1009–17.
15. Couper KN, Blount DG, Wilson MS, Hafalla JC, Belkaid Y, Kamanaka M, Flavell RA, de Souza JB, Riley EM. IL-10 from CD4CD25Foxp3CD127 adaptive regulatory T cells modulates parasite clearance and pathology during malaria infection. *PLoS Pathog* 2008;4:e1000004.
16. Arii S, Sata M, Sakamoto M, Shimada M, Kumada T, Shiina S, Yamashita T, Kokudo N, Tanaka M, Takayama T, Kudo M. Management of hepatocellular carcinoma: Report of Consensus Meeting in the 45th Annual Meeting of the Japan Society of Hepatology (2009). *Hepatol Res* 2010; 40:667–85.
17. Itose I, Kanto T, Kakita N, Takebe S, Inoue M, Higashitani K, Miyazaki M, Miyatake H, Sakakibara M, Hiramatsu N, Takehara T, Kasahara A, et al. Enhanced ability of regulatory T cells in chronic hepatitis C patients with persistently normal alanine aminotransferase levels than those with active hepatitis. *J Viral Hepat* 2009;16:844–52.
18. Kanto T, Hayashi N, Takehara T, Tatsumi T, Kuzushita N, Ito A, Sasaki Y, Kasahara A, Hori M. Impaired allostimulatory capacity of peripheral blood dendritic cells recovered from hepatitis C virus-infected individuals. *J Immunol* 1999;162:5584–91.
19. Mahnke K, Schonfeld K, Fondel S, Ring S, Karakhanova S, Wiedemeyer K, Bedke T, Johnson TS, Storn V, Schallenberg S, Enk AH. Depletion of CD4+CD25+ human regulatory T cells in vivo: kinetics of Treg depletion and alterations in immune functions in vivo and in vitro. *Int J Cancer* 2007;120:2723–33.
20. Ruter J, Barnett BG, Kryczek I, Brumlik MJ, Daniel BJ, Coukos G, Zou W, Curiel TJ. Altering regulatory T cell function in cancer immunotherapy: a novel means to boost the efficacy of cancer vaccines. *Front Biosci* 2009;14: 1761–70.
21. Elrefaei M, Burke CM, Baker CA, Jones NG, Bousheri S, Bangsberg DR, Cao H. HIV-specific TGF-beta-positive CD4+ T cells do not express regulatory surface markers and are regulated by CTLA-4. *Aids Res Hum Retroviruses* 2010;26: 329–37.
22. Han Y, Guo Q, Zhang M, Chen Z, Cao X. CD69+ CD4+ CD25- T cells, a new subset of regulatory T cells, suppress T cell proliferation through membrane-bound TGF-beta 1. *J Immunol* 2009;182:111–20.
23. Li R, Perez N, Karumuthil-Melethil S, Prabhakar BS, Holterman MJ, Vasu C. Enhanced engagement of CTLA-4 induces antigen-specific CD4+CD25+Foxp3+ and CD4+CD25- TGF-beta 1+ adaptive regulatory T cells. *J Immunol* 2007;179:5191–203.
24. Dunham R, Cervasi B, Brenchley JM, Albrecht H, Weintrob A, Sumpter B, Engram J, Gordon S, Klatt NR, Sodora DL, Douek D, Paiardini M, Silvestri G. CD127 and CD25 expression defines $CD4^+$ T cell subsets that are differentially depleted during HIV infection. *J Immunol* 2008; 180:5582–5592.
25. Bengsch B, Spangenberg HC, Kersting N, Neumann-Haefelin C, Panther E, Weizsacker F, Blum HE, Pircher H, Thimme R. Analysis of CD127 and KLRG1 expression on hepatitis C virus-specific $CD8^+$ T cells reveals the existence of different memory T-cell subsets in the peripheral blood and liver. *J Virol* 2007;81: 945–953.
26. Pot C, Jin H, Awasthi A, Liu SM, Lai CY, Madan R, Sharpe AH, Karp CL, Miaw SC, Ho IC, Kuchroo VK. Cutting edge: IL-27 induces the transcription factor c-Maf, cytokine IL-21, and

the costimulatory receptor ICOS that coordinately act together to promote differentiation of IL-10-producing Tr1 cells. *J Immunol* 2009;183:797–801.
27. Chen KJ, Lin SZ, Zhou L, Xie HY, Zhou WH, Taki-Elden A, Zheng SS. Selective recruitment of regulatory T cell through CCR6-CCL20 in hepatocellular carcinoma fosters tumor progression and predicts poor prognosis. *PLOS One* 2011;6:e24671.
28. Zhou J, Ding T, Pan W, Zhu LY, Li L, Zheng L. Increased intratumoralregulatory T cells are related to intratumoral macrophage and poor prognosis in hepatocellular carcinoma patients. *Int J Cancer* 2009;125:1640–8.
29. Bergmann C, Strauss L, Zeidler R, Lang S, Whiteside TL. Expansion and characteristics of human T regulatory type 1 cells in co-cultures simulating tumor microenvironment. *Cancer Immunol Immunother* 2007;56:1429–42.
30. Gregori S, Tomasoni D, Pacciani V, Scirpoli M, Battaglia M, Magnani CF, Hauben E, Roncarolo MG. Differentiation of type 1 T regulatory cells (Tr1) by tolerogenic DC-10 requires the IL-10-dependent ILT4/HLA-G pathway. *Blood* 2010; 116:935–44.
31. Gao Q, Wang XY, Qiu SJ, Yamato I, Sho M, Nakajima Y, Zhou J, Li BZ, Shi YH, Xiao YS, Xu Y, Fan J. Overexpression of PD-L1 significantly associates with tumor aggressiveness and postoperative recurrence in human hepatocellular carcinoma. *Clin Cancer Res* 2009; 15:971–9.
32. Cai MY, Xu YF, Qiu SJ, Ju MJ, Gao Q, Li YW, Zhang BH, Zhou J, Fan J. Human leukocyte antigen-G protein expression is an unfavorable prognostic predictor of hepatocellular carcinoma following curative resection. *Clin Cancer Res* 2009;15:4686–93.

IJC
International Journal of Cancer

Suppression of signal transducers and activators of transcription 1 in hepatocellular carcinoma is associated with tumor progression

Atsushi Hosui[1], Peter Klover[2], Tomohide Tatsumi[1], Akio Uemura[1], Hiroaki Nagano[3], Yuichiro Doki[3], Masaki Mori[3], Naoki Hiramatsu[1], Tatsuya Kanto[1], Lothar Hennighausen[2], Norio Hayashi[4] and Tetsuo Takehara[1]

[1] Department of Gastroenterology and Hepatology, Osaka University Graduate School of Medicine, 2-2 Yamadaoka, Suita, Osaka, Japan
[2] Laboratory of Genetics and Physiology, National Institute of Diabetes and Digestive and Kidney Diseases, National Institutes of Health, Bethesda, MD
[3] Department of Surgery, Osaka University Graduate School of Medicine, 2-2 Yamadaoka, Suita, Osaka, Japan
[4] Kansai-Rosai Hospital, 3-1-69, Inabaso, Amagasaki, Hyogo, Japan

Signal transducers and activators of transcription (STAT) 1 plays a pivotal role in cell-cycle and cell-fate determination, and vascular endothelial growth factor (VEGF) also contributes tumor growth. Recently, interferon (IFN) α has been reported to be effective for prevention of hepatocellular carcinomas (HCCs) recurrence, but the detailed mechanisms remain elusive. *In vitro*, cobalt chloride–treated VEGF induction and hypoxia responsive element (HRE) promoter activity were inhibited by IFNs and this abrogation was cancelled by introduction of small interfering RNA for STAT1. Immunoprecipitation/chromatin immunoprecipitation analyses showed STAT1 bound to hypoxia-inducible factor (HIF)-1α and dissociated HIF-complex from HRE promoter lesion. In a xenograft model using Balb/c nude mice, tumor growth was suppressed by IFNα through inhibition of VEGF expression and it was oppositely enhanced when STAT1-deleted cells were injected. This augmentation was due to upregulation of VEGF and hyaluronan synthase 2. In human samples, 29 HCCs were resected, divided into two groups based on STAT1 activation in tumor and the clinical features were investigated. Patients with suppressed STAT1 activity had a shorter recurrence-free survival. Histological and reverse transcriptase-polymerase chain reaction (RT-PCR) analyses showed portal vein microinvasion and increased VEGF levels in tumors from suppressed STAT1 group. These human samples also showed a reverse correlation between VEGF and STAT1-regulated genes expression. These results *in vitro* and *in vivo* suggested that IFNα are potential candidates for prevention of vessel invasion acting through inhibition of VEGF expression and need to be properly used when STAT1 expression is suppressed.

Key words: STAT1, VEGF, HCC, HIF-1, IFNα

Abbreviations: CH: chronic hepatitis; ChIP: chromatin immunoprecipitation; CoCl2: cobalt chloride; FGF: fibroblast growth factor; HAS: hyaluronan synthase; HCC: hepatocellular carcinoma; HIF: hypoxia-inducible factor; HRE: hypoxia responsive element; IFN: interferon; Ip: Immunoprecipitation; IP: intraperitoneally; IRF: interferon regulatory factor; JAK: Janus kinase; LC: liver cirrhosis; MMP: matrix metalloproteinase; multi: multiple nodular type; NT: adjacent non-tumor tissue; pSTAT: phosphorylated STAT; simple: simple nodular type; STAT: signal transducers and activators of transcription; surr: simple nodule with surrounded proliferation; T: HCC tumors; TIMP: tissue inhibitor of metalloproteinase; TK: thymidine kinase; VEGF: vascular endothelial growth factor
Additional Supporting Information may be found in the online version of this article.

Grant sponsor: Ministry of Education, Culture, Sports, Science, and Technology, Japan
DOI: 10.1002/ijc.27580
History: Received 9 Sep 2011; Accepted 20 Mar 2012; Online 5 Apr 2012

Correspondence to: Tetsuo Takehara, Department of Gastroenterology and Hepatology, Osaka University Graduate School of Medicine, 2-2 Yamadaoka, Suita, Osaka 565-0871, Japan, Tel.: [(81)-6-6879-3621], Fax: +[81-6-6879-3629], E-mail: takehara@gh.med.osaka-u.ac.jp

Introduction

Hepatocellular carcinoma (HCC) is a very common malignancy and causes more than six hundred thousand patients' deaths annually worldwide. The prognosis of HCC is still poor because it often develops with vessel invasion. Several studies have revealed that neovascularization and angiogenic factors, such as vascular endothelial growth factor (VEGF), are significantly upregulated in human HCC samples and play a considerable role in its development and progression.[1]

VEGF contributes to completing vessel invasion and distant metastasis because angiogenesis is thought to be essential for tumor growth. In addition, it is thought that cancer tissues with abundant tumor vessels have many routes of access to distant organs. We are interested not only in the angiogenic potential of VEGF but also in its permeability potential. The permeability function of VEGF appears to strongly involve cancer invasion and metastasis, because high permeability leads to the fragility and opening of cell-to-cell adherence in the vascular endothelium, which might allow the cancer cells to migrate into the vascular lumen.[2]

Interferon (IFN) therapy is frequently used for eradication of hepatitis C virus (HCV) and recently for prevention of HCC recurrence. IFNs are a superfamily of proteins secreted

by human cells that manifest multiple functions in the human body such as protection of cells from viral infection, regulation of cell growth and modulation of the immune system. There are two types of IFN, type 1 IFN (IFNα/β) and type II IFN (IFNγ). The roles of these IFNs against tumor progression and invasion have been reported by several investigators. IFNα inhibits VEGF expression and tumor angiogenesis in neuroendocrine tumors.[3] Qin et al. showed that IFNγ downregulates matrix metalloproteinase (MMP) 2, and Singh et al. presented results showing that IFNα suppresses fibroblast growth factor 2 (FGF2).[4,5] As for signal transducers and activators of transcription (STAT) 1, which is activated by IFNs, genetic polymorphisms in STAT1 gene is reported to associate with increased risk of HCC.[6] In a clinical setting, however, it remains unclear whether and how IFN-STAT signal transduction is associated with tumor progression and vessel invasion. In this study, we investigated the role of IFN-STAT signaling in the process of HCC tumor development using a combination of clinical HCC samples, several HCC cell lines and tumor-transplanted nude mice.

Material and Methods

Cell lines and tissues

Human hepatoma cell lines, PLC/PRF/5, Huh7 and HepG2, were purchased from American Type Culture Collection approximately 3 years ago, and have been tested every year to confirm that their sequences were conserved. They were cultured with Dulbecco's modified Eagle medium supplemented with 10% heat-inactivated fetal bovine serum and treated with various concentrations of IFNα (R&D systems, Minneapolis, MN)/γ (Hayashibara Group, Japan) and/or 100 mM of cobalt chloride ($CoCl_2$; Sigma) and/or 100 ng/ml of IL-6 (R&D systems) or exposed to hypoxia (1% O_2 condition), and then extracted 24 hr after stimulation. To block Janus kinase (JAK)-STAT signal transduction, 100 nM of JAK inhibitor 1, a broad inhibitor of JAKs (Calbiochem, Darmstadt, Germany) or S31-201, specific STAT3 inhibitor (Selleck, TX) was pretreated 1 hr before stimulation. For detection of hydroxylated-hypoxia-inducible factor (HIF)-1α, cells were extracted with lysate buffer including 10 μM of MG132 (Sigma). HCCs and adjacent non-tumor (NT) counterparts were obtained at the time of surgical resection. Written informed consent was provided from each patient. We also obtained the approval of the Ethics committee in Osaka University Graduate School of Medicine.

Plasmid constructs

The pGL2TK plasmid was generated by replacing the SV40 promoter of pGL2 promoter (Promega) with the herpes simplex virus thymidine kinase (TK) promoter fragment (from −105 to +51). The pGL2TkHRE plasmid was kindly provided by Uranchimeg B, National Cancer Institute. In brief, it was produced by subcloning three copies of the HRE (5′-GTGACTACGTGCTGCCTAG-3′) from the iNOS promoter into the pGL2TK promoter vector.[7]

Mice

Balb/c nude mice (CAnN.Cg-Foxn1^{nu}/CrlCrlj) were purchased from Charles River Laboratories (Yokohama, Japan). They were maintained in a specific pathogen-free facility and treated with humane care with approval from the Animal Care and Use Committee of Osaka University Medical School.

Xenograft tumor

To produce a xenograft tumor, 5×10^6 PLC/PRF/5 cells were subcutaneously injected to Balb/c nude mice. For anticancer therapy, 5×10^4 IU/mouse of human IFNα was administrated intraperitoneally (IP) every day, and the same volume of 0.9% saline was injected as a control. Treatment with 10 μg/g BW of bevacizumab (Chugai Pharmaceutical, Japan) IP was started 3 days after injection of HCC cells and was continued three times a week.

Immunoblotting and immunostaining

For immunoblotting, total cellular protein was electrophoretically separated by sodium dodecyl sulfate polyacrylamide gels and transferred onto polyvinylidene difluoride (PVDF) membrane. The membrane was blocked in Tris-buffered saline-Tween containing 5% skim milk for 1 hr and then probed with primary Antibody (Ab) at 4°C overnight. Rabbit monoclonal anti-pSTAT1/STAT1/HIF-1α/hydroxylated HIF-1α Abs and mouse monoclonal anti-STAT3/pSTAT3 Abs were purchased from Cell SignalingTechnology (Beverly, MA). Mouse monoclonal anti-VEGF Ab was from Calbiochem, and anti-CD31 Ab was from R&D systems. Mouse polyclonal anti-β-actin was obtained from Sigma. Horseradish peroxidase-conjugated anti-rabbit or mouse Ab and SuperSignal West Pico System (Pierce, Rockford, IL) were used for the detection of blots.

For immunohistochemistry, tumors were excised and prepared for immunostaining. Tumors were consecutively incubated in PBST for 15 min, in blocking buffer [phosphate-buffered saline with Tween 20 (PBST), 5% normal goat serum, 0.2% bovine serum albumin] for 30 min, in anti-CD31 Ab in blocking buffer for 12 hr, in PBST for 15 min, in Alexa fluor 594 (Molecular Probes, NY) in blocking buffer for an hour, and in PBST for 30 min. Finally, a coverslip was mounted in the mounting medium (Vectashield, Vector Laboratories) with 4′,6-diamidino-2′-phenylindole-dihydrochrolide, and the cells were examined by microscopy.

Protein–protein interaction analysis

To examine the binding of STAT1 protein to HIF-1α protein, immunoprecipitation/western blot analyses were used. The detail procedure is described elsewhere.[8] In brief, from $CoCl_2$ and IFNγ-treated PLC/PRF/5 cells, the cellular protein was extracted and precleared by incubation with protein A-Sepharose beads at 4°C for 1 hr. Next, the sample was incubated with beads coupled to STAT1, pSTAT1, HIF-1α, or hydroxylated-HIF-1α antibody, or rabbit nonspecific γ-globulin (Dako, Denmark) for 18 hr. The immune complex was

eluted by being boiled for 5 min, and finally the supernatant was used for western blot to detect each protein.

Analyses of cell growth

To examine the cell growth curve, 5×10^3 of PLC/PRF/5 cells were seeded on a 96-well culture plate. After 24, 48, 72 and 96 hr, the net number of viable cells was assessed colorimetrically using water-soluble tetrazolium (2-[2-methoxy-4-nitrophenyl]-3-[4-nitrophenyl]-5-[2,4-disulfophenyl]-2*H*-tetrazolium monosodium salt) (Roche Applied Science, IN). This assay is based on cleavage of the tetrazolium salt by mitochondrial dehydrogenase in viable cells. For the assay, 10 μl of the water-soluble tetrazolium reagent was added to the 100-μl culture medium, followed by the incubation at 37°C for 1 hr. The optical density at 450 nm was measured. The assay was done in quadruplicate and the values were expressed as the means ± S.D.

ChIP

Chromatin immunoprecipitation (ChIP) analysis was basically performed according to the manufacturers' instructions of MAGnify ChIP System (Invitrogen). In brief, cells (~5.0×10^7) were grown to a confluencey of 85–90% in complete media and treated with 100 μM $CoCl_2$ for 24 hr. These cells were treated with 1% formaldehyde for 10 min at room temperature, followed by the addition of 1.25 M glycine to a final concentration of 0.125 M. Cells were washed in 4°C PBS and pelleted in 1 ml of lysis buffer with protease inhibitors and incubated for 10 min at 4°C. Nuclear lysates were sonicated (Sonifier 250, Branson) for 15 cycles of 30 sec ON and 30 sec OFF to shear DNA to 200–500 bp fragments. Chromatin solutions were precleared and incubated with anti-HIF-1α, STAT1 or the nonspecific γ-globulin (negative control) and rotated overnight at 4°C. Chromatin/protein complex was purified and applied to PCR analysis. The region −1,386 to −1,036 of the VEGF promoter was PCR amplified from the immunoprecipitated chromatin using the following primers: sense 5′-CAGGTCAGAAACCAGCCAG, antisense; 5′-CGTG ATGATTCAAACCTACC. The 350-bp PCR product was resolved on a 1.2% agarose gel and visualized by ethidium bromide staining and UV illumination.

RNA extraction, real-time PCR analysis and small RNA interference

Total RNA was isolated (miRNeasy Mini Kit, Qiagen, Valencia, CA), reverse-transcribed (High Capacity RNA-to-cDNA Master Mix, Applied Biosystems) and then applied to real-time PCR analysis (TaqMan Gene Expression Assays, Applied Biosystems) normalized to beta-actin expression levels. All measurements were performed in triplicate. The details of each probe for real-time PCR are described in Table 1, Supporting Information. Cells were transfected with Stealth select RNA interference (RNAi, set of three oligonucleotides, Invitrogen) directed against STAT1. A Stealth RNAi negative control kit (set of three oligonucleotides, Invitrogen) was used as a control for sequence-independent effects following Stealth RNAi delivery. The transfections were carried out using Lipofectamine RNAiMAX (Invitrogen) according to the reverse transfection protocol.

Quantitative analysis of hyaluronic acid

Hyaluronic acid enzyme-linked immunosorbant assay (ELISA) kit was purchased from Biotech Trading Partners (NY). Each assay was performed according to the manufacturer's instructions. In brief, the removed subcutaneous tumors were dried and treated with pronase E for 24 hr. The product was boiled for 10 min and centrifuged, and the supernatants were subjected to ELISA assay.

Statistical analysis

Data were presented as mean ± standard error (SE) (for *in vivo* experiments) or as mean ± standard deviation (for *in vitro* experiments). Comparisons between the two groups were performed by the unpaired *t*-test. Multiple comparisons were performed by ANOVA with the Scheffe post hoc test. Recurrence-free survival curves were estimated using the Kaplan-Meier method. $p < 0.05$ was considered statistically significant.

Results

IFNα suppresses VEGF expression through inhibiting HRE-promoter activity

To clarify the relationship between STAT1 activity and VEGF expression in HCC, we used a hypoxia model to induce VEGF expression, and treated HCC cell lines with IFNα, which is known to activate STAT1.[9] This hypoxia model mimics the clinical setting of HCC, which was done by administration of $CoCl_2$. Our results shown in Figure 1*a* were compatible with previous reports, suggesting that both $CoCl_2$ and IFNα worked well in this experiment using PLC/PRF/5 cells. VEGF mRNA/protein expression was enhanced by $CoCl_2$, but this induction was inhibited by IFNα administration in a dose-dependent manner. This inhibitory effect was cancelled by introduction of JAK inhibitor or STAT1 knockdown (Figs. 1*b* and 1*c*). HepG2 and Huh7 cells were both used and displayed the same tendencies as these results (Fig. 1, Supporting Information). VEGF expression is regulated by the heterodimeric HIF-1, which is made up of HIF-1α and HIF-1β to the hypoxia responsive elements (HRE) on several target genes. HIF-1β is constitutively expressed irrespective of various conditions, but HIF-1α is proline-hydroxylated leading to a conformational change that promotes ubiquitination and proteasomal degradation under normoxic conditions.[10] We next tried to find how $CoCl_2$-induced VEGF induction was suppressed by IFNα stimulation by examining the expression levels of HIF-1α and hydroxylated HIF-1α. $CoCl_2$ induced HIF-1α expression, and this induction level was not altered by IFNα treatment (Fig. 1*d*). Hydroxylated HIF-1α was expressed at low levels with or without $CoCl_2$ and/or IFNα. This inhibitory effect of

Table 1. Demographic characteristics of patients and tumors

	Total HCC patients	Suppressed pSTAT1 group	control group
Total number	29	7	22
Male/Female	21/8	6/1	15/7
Age (year)	61.6 ± 10.3	66.5 ± 8.0	60.2 ± 10.8
Etiology (HBV/HCV)	11/15	3/5	8/10
NT lesion (normal/CH/LC)	2/18/9	0/6/1	2/12/8
ALT	44.0 ± 30.0	41.1 ± 21.0	46.2 ± 33.2
Platelets	15.7 ± 5.8	14.7 ± 1.9	16.0 ± 5.6
Child (A/B/C)	20/3/6	7/0/0	13/3/6
Stage (I/II/III/IV)	2/16/10/1	0/6/1/0	2/10/9/1
HCC recurrence (within/over 2 years)	15/14	7/0 *1	8/14
Tumor size (cm)	4.8 ± 2.6	5.5 ± 2.4	4.6 ± 2.3
Macroscopic classification (simple/surr/multi/invasive)	6/13/6/4	1/5/0/1	5/8/6/3
Capsule formation (+/−)	20/9	7/0 *2	13/9
Histology (moderate/poor)	10/19	3/4	7/15
AFP	1337 ± 4402	766 ± 579	1637 ± 5161
Vessel invasion (Vv +/−)	1/28	0/7	1/21
Vessel invasion (Vp +/−)	9/20	5/2 *3	4/18

Liver function was categorized by Child-Pugh classification and the tumors were also staged by means of the pTNM system. At least every 3 months, diagnostic imaging and blood sampling was done to check for HCC recurrence. Asterisks indicate significant differences (*1, $p = 0.0033$, *2, $p = 0.042$, *3, $p = 0.008$).

IFNα on VEGF expression was also seen in low O_2 condition (Fig. 2, Supporting Information). Next, HRE promoter activity was assessed by transfection of the luciferase construct (pGL2TkHRE) that included HRE and the minimal promoter TK gene upstream of the luciferase gene.[7,11] As shown in Figure 1*e*, HRE promoter activity was enhanced by treatment with $CoCl_2$, and this upregulation was inhibited by IFNα stimulation. This inhibitory effect was abolished by introducing STAT1 siRNA as is the case with VEGF expression. IFNγ has also the same inhibitory effect on VEGF expression as IFNα (Fig. 3, Supporting Information). Our results, therefore, show that activation of JAK-STAT1 signal transduction causes inhibition of VEGF expression through suppression of HRE promoter activity.

STAT1 forms a complex with HIF-1α

We hypothesized that a direct interaction of STAT1 and HIF-1 could be responsible for the effect of pSTAT1 on formation of the HIF-1 complex or on its binding to HRE. To test this, we examined the binding of STAT1 to HIF-1 protein by means of immunoprecipitation (Ip)/western blot analysis (Fig. 1*f*). From $CoCl_2$ and IFNγ-treated PLC/PRF/5 cells, the cellular protein was extracted and applied to Ip assay. The HIF-1α protein was not found in the negative control using nonspecific γ-globulin (*lane 1*) but detected in the immunoprecipitates using antibodies against pSTAT1 (*lane 2*) and STAT1 (*lane 3*). In similar fashion, STAT1 protein was seen in the immunoprecipitates using antibodies against HIF-1α. These findings indicate the possible binding of HIF-1α protein to STAT1 protein. To further determine if this interaction has an effect on binding of the HIF-1 complex to HRE, we performed *in vitro* ChIP assays. Cultured cells were treated with $CoCl_2$ in the absence (Fig. 1*g*, *lanes 1, 4*) or presence of IFNγ (*lanes 2, 5*). Before these treatments, STAT1 expression was knocked down by siRNA (*lanes 3, 6*). The PCR product designed within HRE was not found in the negative control sample using nonspecific γ-globulin (*lanes 1-3*) but detected in the immunoprecipitates using antibodies against HIF-1α (*lanes 4-6*). The detection level was less in IFNα-treated cells, and this inhibitory effect was canceled in STAT1-deleted cells. No bands were seen in immunoprecipitates using STAT1 antibodies (lane 7) though STAT1 binds to HIF-1α complex and then might be associated with HRE. These results indicate that STAT1 bound to HIF-1α protein, and this binding caused the HIF-1α complex disassociate with HRE.

IFNα has an inhibitory effect on tumor development in the presence of STAT1 but an opposite effect in the absence of STAT1

Several investigators have already reported that IFNα has antiproliferative effects by inhibiting cell-cycle progression or by inducing apoptosis.[12,13] *In vitro*, the growth of cultured cells were inhibited by IFNα stimulation irrespective of STAT1, indicating that antiproliferative effects involve both STAT1-dependent and -independent mechanisms (Fig. 4, Supporting Information). To clarify the relationship between IFNα-STAT1 and VEGF *in vivo*, we developed a xenograft model using nude mice. STAT1 gene knock down by siRNA

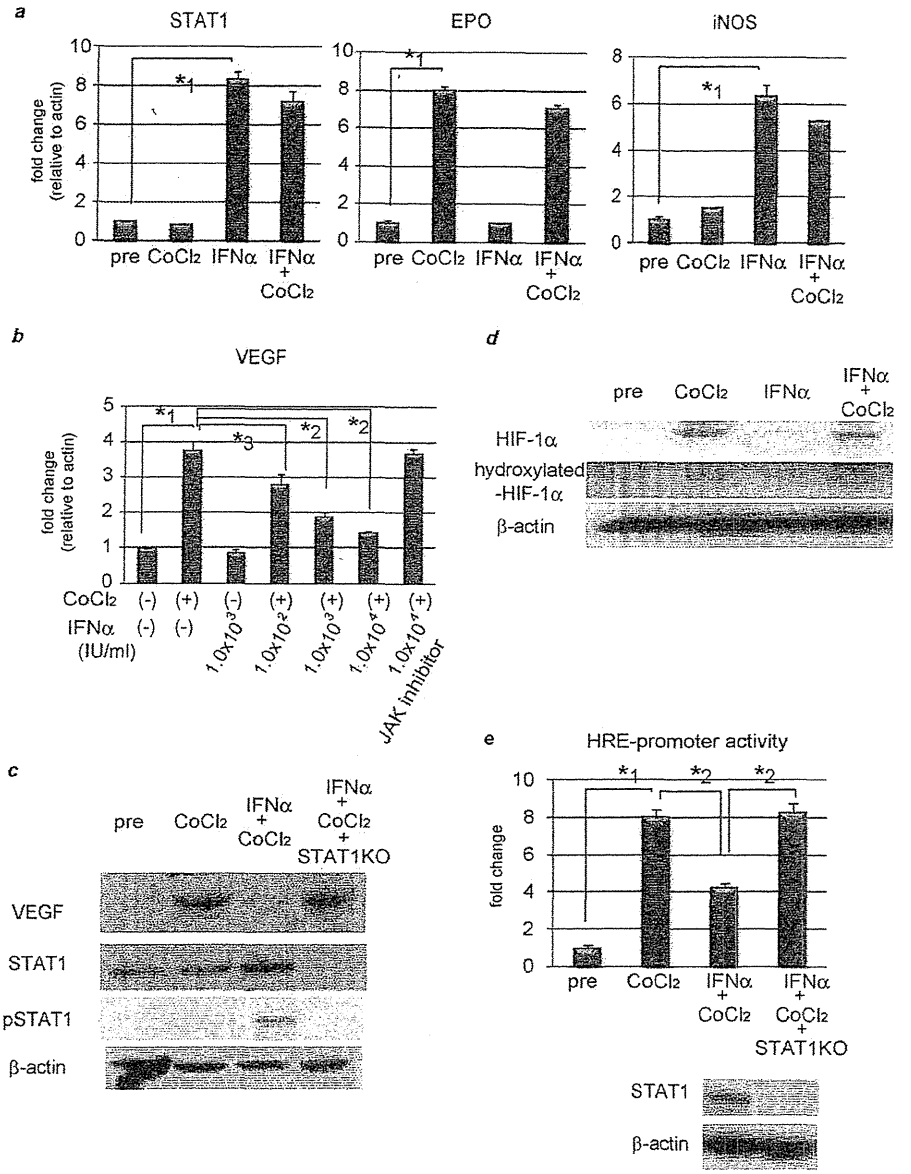

Figure 1. IFNα suppresses VEGF expression through inhibiting HRE-promoter activity by interaction between STAT1 and HIF-1 complex. (*a*, *b*) Expression levels as detected by real-time RT-PCR analysis. Cells were treated with 100 μM $CoCl_2$ and/or 1.0×10^3 IU/ml (*a*) or various concentrations of IFNα (*b*) for 24 hr. To block JAK-STAT signal transduction, 100 nM of JAK inhibitor 1 was pretreated 1 hr before stimulation. (*c*) Activation of STAT1 and expression of STAT1 and VEGF as detected by western blot analysis. PLC/PRF/5 cells were transfected with control siRNA or siRNA for STAT1 and subjected to each stimulation for 24 hr. (*d*) Expression levels of HIF-1α and hydroxylated-HIF-1α as detected by western blot analysis. (*e*) Cells were cotransfected of the pGL2TkHRE plasmid or the pGL2Tk plasmid (as a control vector) with the pRLtK plasmid (Promega). The cells were then stimulated with 100 mM of $CoCl_2$ units/ml and/or 1.0×10^3 IU/ml of IFNα, or left unstimulated, and subjected to dual luciferase assay. The relative light unit of the unstimulated sample was considered as 1 and the data were expressed as mean ± S.D. Lower panel shows expression levels of STAT1 as detected by western blot analysis. (*f*) Cellular lysates from $CoCl_2$ and IFNγ-treated PLC/PRF/5 cells were immunoprecipitated with nonspecific γ-globulin (*lane 1*) and antibodies against pSTAT1 (left panel, *lane 2*), STAT1 (left panel, *lane 3*), HIF-1α (right panel, *lane 2*), and hydroxylated-HIF-1α (right panel, *lane 3*), and the immunoprecipitates were subjected to western blot analysis to detect each protein. (*g*) ChIP assay with HIF1α or STAT1 antibody. Cells were transfected with siRNA for STAT1 or control, and stimulated with $CoCl_2$ for 24 hr and/or IFNα for 3 hr. The immunoprecipitated DNA was purified and the region from −1386 to −1036 base pairs of the human VEGF promoter was amplified by PCR (35 cycles). Cell lysates without Ip was used as a positive control (lane 8). Asterisks indicate significant differences (*1, $p < 0.001$, *2, $p < 0.01$, *3, $p < 0.05$).

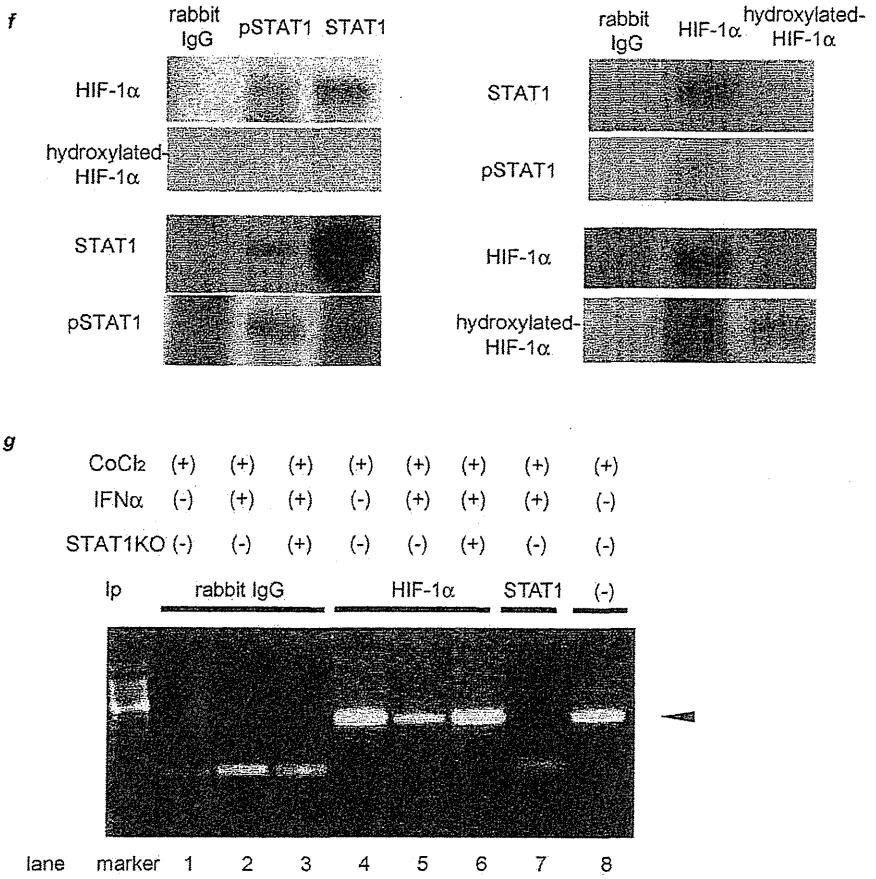

Figure 1. (Continued)

was tested for reduction of STAT1 levels in several hepatoma cell lines. Western blot analysis showed STAT1 expression had been reduced by this method for more than 20 days, and that it was most efficient in PLC/PRF/5 cells (Fig. 5, Supporting Information). Several nude mice were then subcutaneously injected with control and STAT1-deleted cells to form xenograft tumors and were randomly assigned into two groups; one was treated with human IFNα, and the other with 0.9% saline as the control. In the presence of STAT1, IFNα had a strong inhibitory effect on the tumor development as expected, but in the absence of STAT1, surprisingly, IFNα had the opposite effect, that is, it enhanced tumor growth (Fig. 2*a*). Without IFNα treatment, there was no significant difference in tumor growth between control and STAT1-deleted cells. We also confirmed that STAT1 expression in tumor had been knocked down for at least 20 days after injection (Fig. 2*b*). Real-time RT-PCR and western blot analyses revealed that VEGF expression in tumors resected 20 days after transplantation was lower in the IFNα-treated group than in the control, which was consistent with the *in vitro* results, but surprisingly it was increased when the STAT1 gene was knocked down (Figs. 2*c* and 2*d*). To examine whether inhibition or progression of tumor growth was due to VEGF levels, we used bevacizumab, a VEGF monoclonal antibody, and measured tumor size at 25 days after injection of tumor cells. No differences were noted between the control and IFNα-treated groups irrespective of STAT1 expression when these mice were treated with bevacizumab (Fig. 2*e*). To examine the possibility that the human IFNα acts *in vivo* equally well on mouse cells and on human cell lines, we extracted mouse liver as well as transplanted tumor and examined STAT1 activity. It revealed that STAT1 was strongly activated in human cell lines but less activated in mouse liver (Fig. 6, Supporting Information). These data suggest that in this model, IFNα had an inhibitory effect on tumor growth through inhibition of VEGF expression, and that it also had a promotive effect through enhancement of VEGF expression when STAT1 expression was knocked down in tumor cells.

As a typical hypervascular tumor, HCC produces and secretes VEGF, thereby forming new tumor vessels, which provide oxygen and nutrients to cancer cells causing them to grow. Microvessel density was assessed by CD31 immunostaining of hepatic tumors resected 25 days after injection of tumor cells. It revealed that the number of CD31 positive cells,

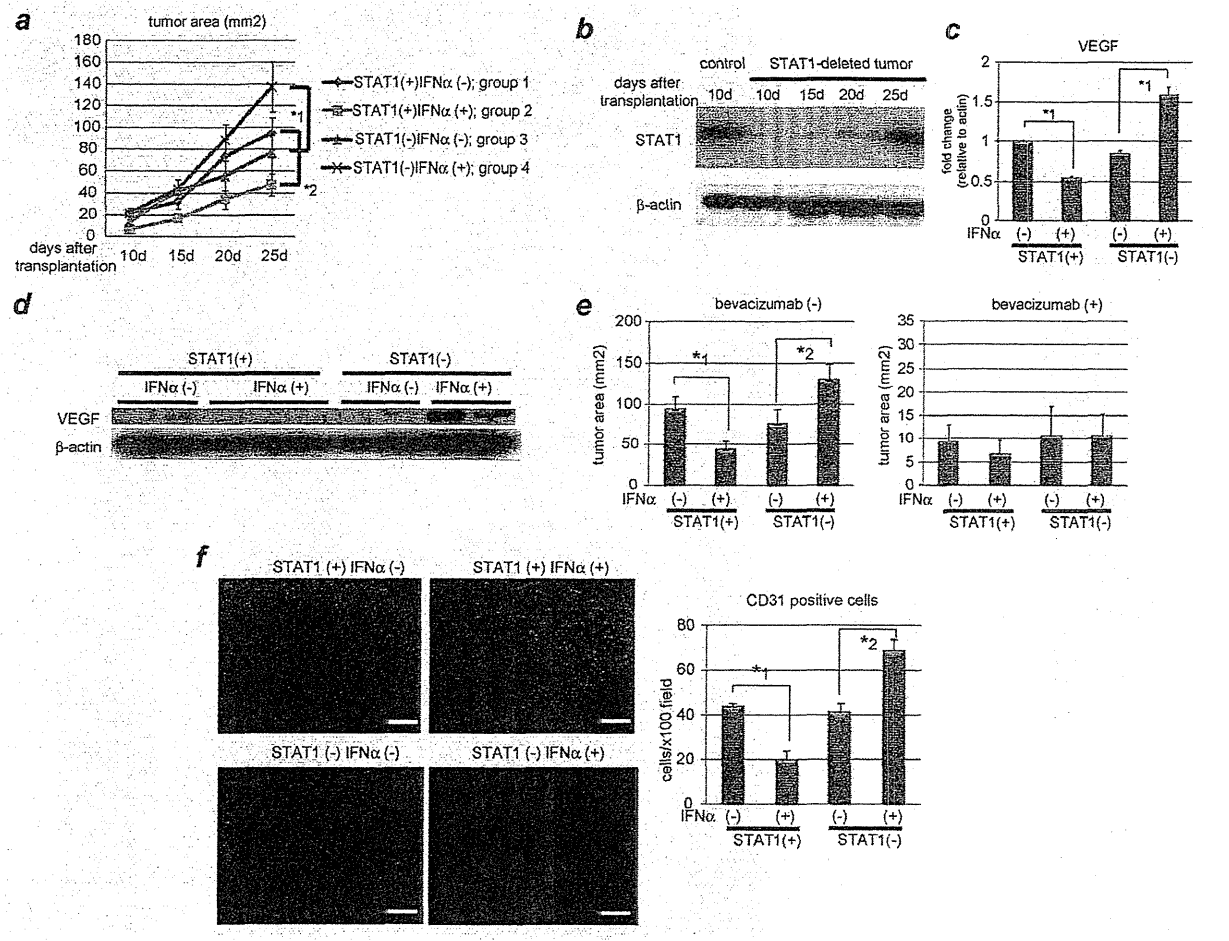

Figure 2. IFNα has an inhibitory effect on tumor development in the presence of STAT1 but an opposite effect in the absence of STAT1. (*a*) PLC/PRF/5 cells were transfected with control siRNA (group 1 and 2) or siRNA for STAT1 (group 3 and 4). One day after treatment, 5×10^6 of these cells were subcutaneously injected to Balb/c nude mice, and tumor area was measured every 5 days. In two groups (group 2 and 4), 5×10^4 IU/mouse of IFNα were administered IP every day, and in the other groups (group 1 and 3) the same volume of 0.9% saline was injected as a control. The number of mice in each group was 5–7. (*b*) Expression levels of STAT1 as detected by western blot analysis. Each subcutaneous tumor in group 4 was removed at the different time points (10, 15, 20 25 days after transplantation). One of tumors in group 2 was used as a positive control. (*c, d*) Expression levels of VEGF as detected by real-time RT-PCR or western blot analysis. Each subcutaneous tumor was removed 20 days after transplantation. (*e*) Tumor area at 25 days after transplantation in each group in the absence (left panel) or presence (right panel) of bevacizumab, the monoclonal anti-VEGF antibody ($N = 5–7$ per group). Three days after injection of tumor cells, 10 mg/g body weight of bevacizumab were injected IP twice a week. (*f*) Immunofluorescent staining with anti-CD31 (red) antibody and Dapi (blue). Images are shown at low magnification (100×, left panel). Bars, 200 μm. The number of CD31-positive cells were presented (right panel). These data were acquired from three different fields in each tumor. Asterisks indicate significant differences (*1, $p < 0.01$, *2, $p < 0.05$).

as an indicator of microvessels, was less in IFNα-treated mice, but without STAT1 they were enhanced by IFNα administration (Fig. 2*f*). Taken together, IFNα plays contrary roles for forming tumor vessels by regulating VEGF expression.

IFNα regulates VEGF expression through STAT3 activation in STAT1-null cells

Tumor growth was seen only in the STAT1-deleted and IFNα-treated group even when 1×10^5 cells were injected, although no tumors were observed in the other groups (Fig. 3*a*). Some adhesion molecules were examined and hyaluronan synthase (HAS) 2 was induced by IFNα stimulation in the STAT1-deleted cells and higher expression levels of hyaluronic acid were observed in the STAT1-deleted and IFNα-treated tumors (Figs. 3*b* and 3*c* and Fig. 7, Supporting Information). The presence of STAT1 has an effect on them because HAS2 expression and HA concentration were also different between STAT1 (−);IFN (−) group and STAT1(−); IFN (−) group. These results indicate that IFNα-STAT1 regulates HAS2 expression, promoting attachment of tumor cells, because HAS2 has been implicated in the developmental process involving adherence to the extracellular matrix

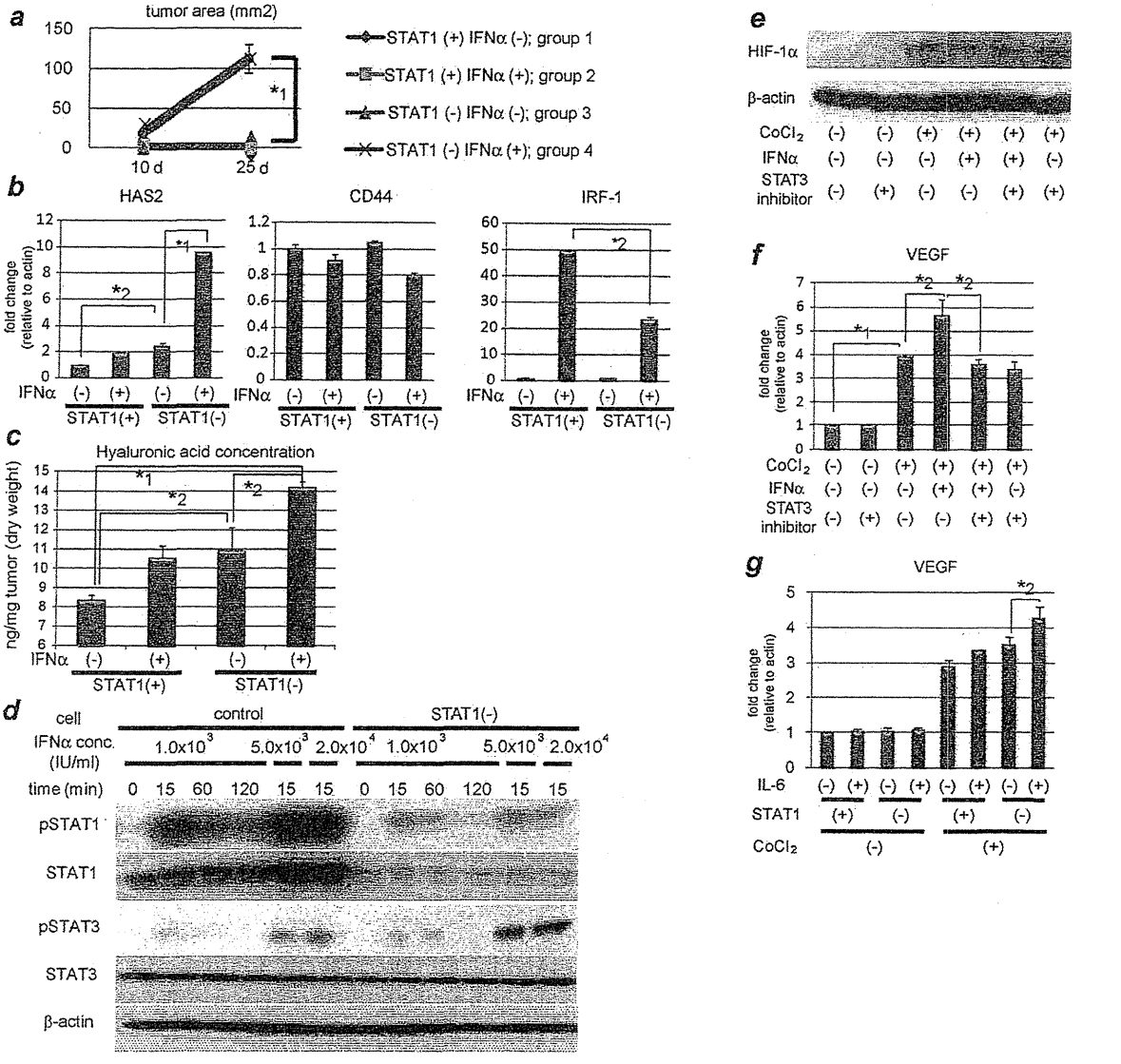

Figure 3. IFNα causes enhancement of HAS2 and VEGF through STAT3 activation in the absence of STAT1. (*a*) 1×10^5 of transfected cells were subcutaneously injected to Balb/c nude mice. Other procedures are the same as *b*. (*b*) Expression levels of hyaluronic acid synthase (HAS) 2, CD44 and IRF-1 as detected by real-time RT-PCR analysis. PLC/PRF/5 cells were transfected with control siRNA or siRNA for STAT1 and stimulated on the next day with 5.0×10^3 IU/ml of IFNα for 3 hr or left untreated. (*c*) Hyaluronic acid levels of each tumor as detected by ELISA assay. (*d*) Activation/expression of STAT1 and STAT3 as detected by western blot analysis. PLC/PRF/5 cells were transfected with control siRNA or siRNA for STAT1 and stimulated on the next day with various concentration of IFNα for 15, 60, or 120 min. (*e*, *f*) STAT1-knockdown cells were pretreated with or without 100 μM of S31-201, a specific STAT3 inhibitor, before $CoCl_2$ and/or 5.0×10^3 IU/ml of IFNα. (*e*) Expression levels of HIF-1α as detected by western blot analysis. (*f*, *g*) Expression levels of VEGF as detected by real-time RT-PCR analysis. (*g*) Control and STAT1-knockdown cells were treated with $CoCl_2$ and/or 100 ng/ml of IL-6. Asterisks indicate significant differences (*1, $p < 0.001$, *2, $p < 0.01$).

and tissue expansion through high expression of hyaluronic acid.[14]

The inhibitory effect of STAT1 on VEGF expression was due to its binding to HIF-1α, but the enhancement effect remains unclear. Jung et al.[15] have reported that STAT3 is a potential modulator of HIF-1-mediated VEGF expression. To examine STAT3 activation under IFNα stimulation, western blot analysis was performed. As shown in Figure 3*d*, 1.0×10^3 IU/ml of IFNα induced almost the same level of phosphorylated STAT3 (pSTAT3), but prolonged STAT3 activity more in the STAT1-deleted cells than in the control. Administration of a higher concentration of IFNα, such as 5.0×10^3 or 2.0×10^4 IU/ml, also caused much more activation of STAT3 in the STAT1 knock-down cells than in the control.

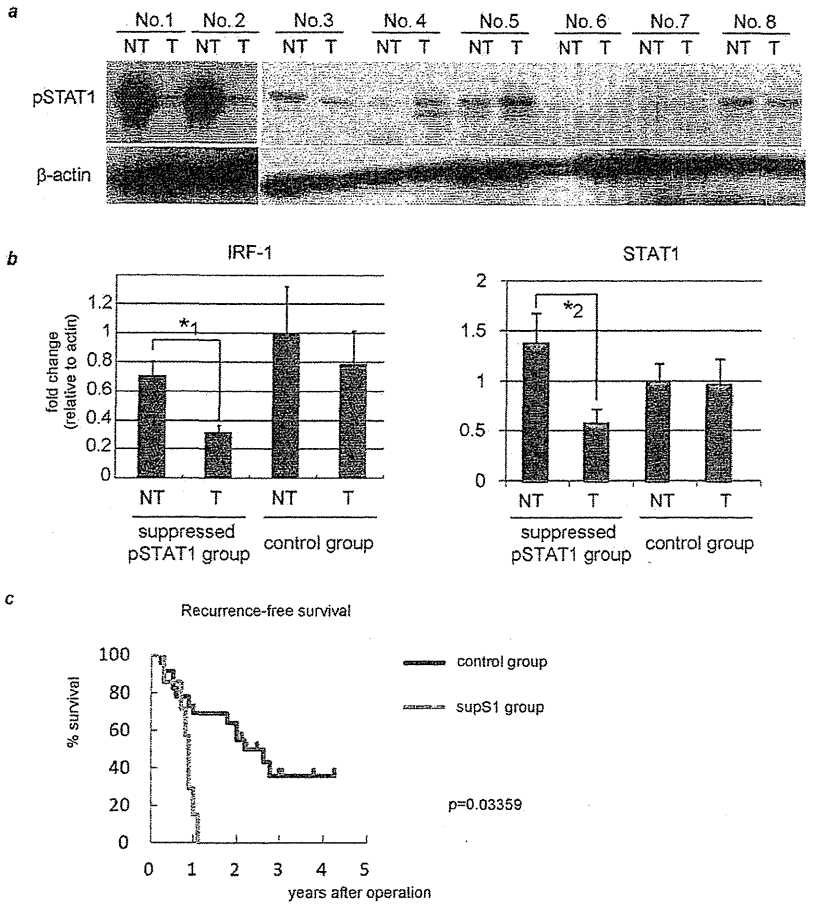

Figure 4. Suppressed STAT1 activity links to upregulation of VEGF, which might cause early HCC recurrence. Twenty-nine pairs of surgically resected human HCC tumors (T) and adjacent NT tissues were used. They were divided into two groups based on STAT1 activity (supS1 versus control). (*a*) Activation levels of STAT1 in T and NT as detected by western blot analysis. Representative data are presented. (*b, d*) Expression levels in each tissue of two divided groups as detected by real-time RT-PCR analysis. The relative expression level of the NT sample in the control group was set as 1, and the fold expression level of each tissue was calculated. (*c*) Predictors of recurrence-free survival were identified using the Kaplan-Meier method. (*e*) IRF-1, STAT1, and VEGF mRNA levels in the liver of 29 HCC samples were determined by real-time RT-PCR and plotted to analyze the correlation between IRF-1 and VEGF (Pearson correlation coefficient (R) = −0.5446, $p < 0.01$) (left) or between STAT1 and VEGF ($R = -0.5514$, $p < 0.01$) (right). The asterisks indicate significant differences (*1, $p < 0.01$, *2, $p < 0.05$, *3, $p < 0.05$ versus all other groups).

These data indicate that IFNα activated STAT3 without de novo protein synthesis, which might result in high expression of VEGF when STAT1 expression has been knocked down. The influence of enhanced STAT3 activity on HIF-1α expression in the STAT1 knock-down cells was examined by western blot analysis but IFNα had no effects on HIF-1α expression, irrespective of S31-201, specific STAT3 inhibitor (Selleck, TX)(Fig. 3*e*). Administration of $CoCl_2$ induced VEGF expression and this induction was enhanced by IFNα stimulation in STAT1-null cells (Fig. 3*f*). This augmentation was canceled by pretreatment with S31-201, providing evidence that IFNα enhanced VEGF expression through STAT3 activation in the absence of STAT1. This synergistic effect was found not only with $CoCl_2$ and IFNα stimulation, but also with $CoCl_2$ and IL-6 stimulation (Fig. 3*g*). These results indicate that inflammation itself is a potent modulator of VEGF expression when STAT1 expression is silenced or downregulated.

Patients with suppressed STAT1 activity show a poor prognosis, which might be linked to upregulation of VEGF

To examine the activity of STAT1 in human HCC samples, we used 29 pairs of surgically resected human HCC tumors (T) and adjacent NT tissue samples. The backgrounds of the 29 cases are shown in Table 1. No one had received radiation or chemotherapy after surgery. In seven cases, STAT1 phosphrylation was suppressed in T compared to NT while in two cases, it was enhanced. All cases were then divided into two groups. In suppressed STAT1 group, STAT1 activity level was reduced more than by two-fold in T to NT by

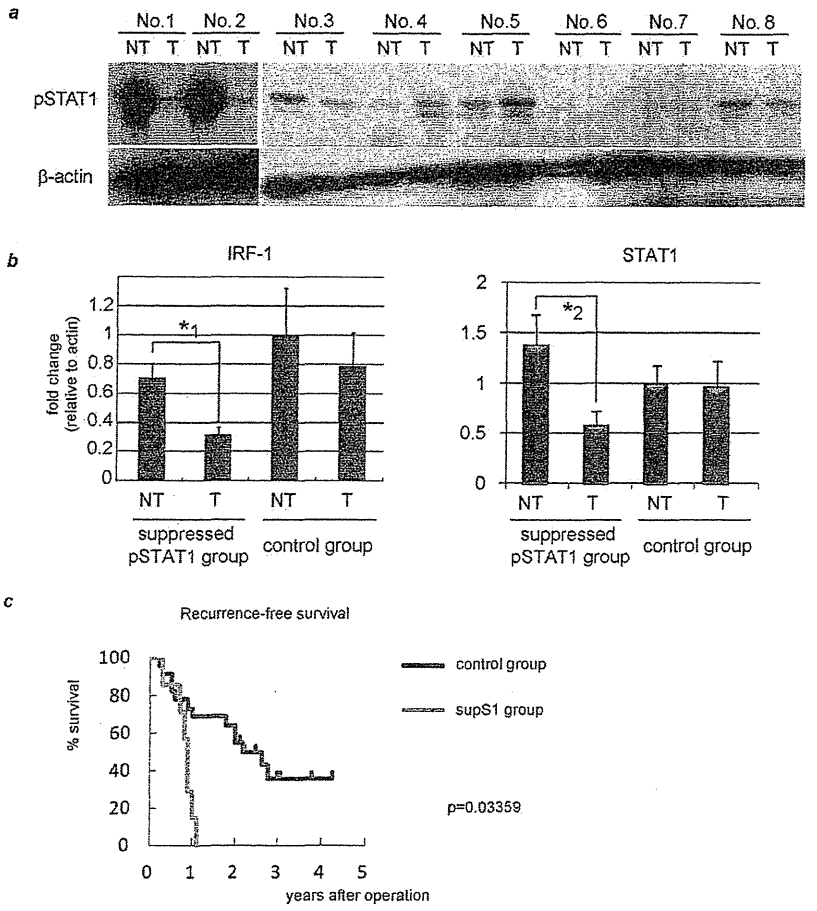

Figure 4. (Continued)

western blot (abbreviated as supS1 group, representative data was shown in Fig. 4*a*, No. 1 and 2). In 22 patients, STAT1 activation was not so changed or enhanced when comparing T with NT (control group, Fig. 4*a*, No. 3–8). These two groups had no statistical differences in their clinical backgrounds (Table 1). With most the same levels of serum alanine aminotransferase, our results suggest that these two groups had similar levels of hepatic inflammation. Expression of STAT1 target genes, such as interferon (IFN) regulatory factor (IRF)-1 and STAT1 itself, were measured by real-time RT-PCR, and statistically less expression of these molecules in the supS1 group were found in T than in NT (Fig. 4*b*). This is evidence for STAT1 activation in the supS1 group being suppressed in HCC tissues. Next, prognostic factors were examined, and surprisingly, all patients in the supS1 group displayed HCC recurrence within 2 years irrespective of having the same levels of liver function and staging of HCC compared to the control group (Table 1). We also observed suppression of STAT1 activity in tumor was associated with significantly worse recurrence-free survival by Kaplan-Meir analysis (Fig. 4*c*). As for the cause of the early recurrence in the supS1 group, the rate of microscopic portal venous invasion was significantly higher in the supS1 group. This finding indicates that the early recurrence may be associated with microportal invasion.

We next asked why suppression of hepatic STAT1 activity could be linked to vessel invasion by examining vessel invasion-related molecules, such as FGF, MMP, tissue inhibitor of metalloproteinase and VEGF, in these two subject groups. VEGF expression level was higher in the whole supS1 group than in the control, and its expression is much more enhanced in T than in NT (Fig. 4*d* and Fig. 8, Supporting Information). Other molecules were supposed not to contribute to the high HCC recurrence in supS1 group. Not only angiogenic potential but also permeability functions of VEGF appear to strongly mediate cancer invasion as described in the Introduction section.[2,16] These results and previous reports suggest that inhibited STAT1 activity might cause up-regulation of VEGF expression, resulting in portal invasion and poor prognosis.

To investigate finally the direct regulation of VEGF by STAT1 activation, we used these HCC samples. They

revealed a reverse correlation between VEGF and STAT1-regulated gene expression, such as IRF-1 and STAT1 itself (Fig. 4*e*). As the number of patients in this study was quite small, we cannot come to the strong conclusion, but these results are consistent with the hypothesis that STAT1 activation negatively regulates VEGF expression.

Discussion

Recently, IFNα therapy has been reported to be effective for preventing HCC recurrence.[17] IFN is known to exert immunomodulatory effects by stimulating T cells, natural killer cells and monocytes. These immune cells play roles in prevention of HCC recurrence by IFNα therapy, however, it remains elusive whether IFNα therapy is effective on hepatocytes, and how IFNα mediates its effect on them.

We have shown *in vitro* that IFNα-treated activation of JAK-STAT pathway causes inhibition of VEGF expression through abrogation of HRE-promoter activity. Some molecules were reported to have effects on gene transcription of VEGF,[3,18] but this is the first report to show that STAT1 directly binds to HIF-1 and regulates HRE-promoter activity. This is a newly discovered mechanism about IFNα-treated inhibition of VEGF expression, but more important is the fact that IFNα has adverse effects when STAT1 expression is silenced. That is, STAT3 is much more activated under stimulation with IFNα, followed by enhancement of expression of target genes, such as VEGF, as indicated in this study. This is the so-called "STAT-shift," and the same event occurs in the case of the growth hormone-STAT5, interleukin-6-STAT3.[19–21] STAT1 expression is regulated by IFNα, and thus the less activated the STAT1 is, the less it is expressed. This negative loop of STAT1 is more likely to occur in the clinical setting than other STATs. In some cases, IFNα therapy causes rapid progression of HCC with vessel invasion,[22] in which case the molecular pathogenesis might be explained by a STAT-shift and negative loop of STAT1 action.

This study has yielded three novel findings. First, patients with suppressed STAT1 activity have poor prognosis because of high HCC recurrence. This might be caused by upregulation of VEGF. Second, IFNα-treated activation of JAK-STAT pathway causes inhibition of VEGF expression through interaction of the HIF-1 complex with STAT1. Third, treatment with IFNα contributes to the harmful consequences when STAT1 expression is silenced or downregulated. These findings should be helpful for deciding which therapy is suitable for HCC patients. In some cases, conventional therapy should be replaced by other therapies, such as bevacizumab, one of the molecular target drugs for patients with suppressed STAT1 activity in tumor.

Acknowledgements

The authors are grateful to Badarch Uranchimeg (National Cancer Institute) for providing us with the pGL2TkHRE plasmid. They also thank Wei Li for technical assistance.

References

1. Mise M, Arii S, Higashituji H, et al. Clinical significance of vascular endothelial growth factor and basic fibroblast growth factor gene expression in liver tumor. *Hepatology* 1996;23:455–64.
2. Poon RT, Ng IO, Lau C, et al. Serum vascular endothelial growth factor predicts venous invasion in hepatocellular carcinoma: a prospective study. *Ann Surg* 2001;233:227–35.
3. von Marschall Z, Scholz A, Cramer T, et al. Effects of interferon alpha on vascular endothelial growth factor gene transcription and tumor angiogenesis. *J Natl Cancer Inst* 2003;95:437–48.
4. Qin H, Moellinger JD, Wells A, et al. Transcriptional suppression of matrix metalloproteinase-2 gene expression in human astroglioma cells by TNF-alpha and IFN-gamma. *J Immunol* 1998;161:6664–73.
5. Singh RK, Gutman M, Bucana CD, et al. Interferons alpha and beta down-regulate the expression of basic fibroblast growth factor in human carcinomas. *Proc Natl Acad Sci USA* 1995;92:4562–6.
6. Zhu ZZ, Di JZ, Gu WY, et al. Association of genetic polymorphisms in STAT1 gene with increased risk of hepatocellular carcinoma. *Oncology* 2011;78:382–8.
7. Rapisarda A, Uranchimeg B, Scudiero DA, et al. Identification of small molecule inhibitors of hypoxia-inducible factor 1 transcriptional activation pathway. *Cancer Res* 2002;62:4316–24.
8. Hosui A, Ohkawa K, Ishida H, et al. Hepatitis C virus core protein differently regulates the JAK-STAT signaling pathway under interleukin-6 and interferon-gamma stimuli. *J Biol Chem* 2003;278:28562–71.
9. Shuai K, Horvath CM, Huang LH, et al. Interferon activation of the transcription factor Stat91 involves dimerization through SH2-phosphotyrosyl peptide interactions. *Cell* 1994;76:821–8.
10. Maxwell PH, Wiesener MS, Chang GW, et al. The tumour suppressor protein VHL targets hypoxia-inducible factors for oxygen-dependent proteolysis. *Nature* 1999;399:271–5.
11. Melillo G, Musso T, Sica A, et al. A hypoxia-responsive element mediates a novel pathway of activation of the inducible nitric oxide synthase promoter. *J Exp Med* 1995;182:1683–93.
12. Yano H, Iemura A, Haramaki M, et al. Interferon alfa receptor expression and growth inhibition by interferon alfa in human liver cancer cell lines. *Hepatology* 1999;29:1708–17.
13. Dunn C, Brunetto M, Reynolds G, et al. Cytokines induced during chronic hepatitis B virus infection promote a pathway for NK cell-mediated liver damage. *J Exp Med* 2007;204:667–80.
14. Udabage L, Brownlee GR, Nilsson SK, et al. The over-expression of HAS2, Hyal-2 and CD44 is implicated in the invasiveness of breast cancer. *Exp Cell Res* 2005;310:205–17.
15. Jung JE, Lee HG, Cho IH, et al. STAT3 is a potential modulator of HIF-1 mediated VEGF expression in human renal carcinoma cells. *FASEB J* 2005;19:1296–8.
16. Schmitt M, Horbach A, Kubitz R, et al. Disruption of hepatocellular tight junctions by vascular endothelial growth factor (VEGF): a novel mechanism for tumor invasion. *J Hepatol* 2004;41:274–83.
17. Nagano H. Treatment of advanced hepatocellular carcinoma: intraarterial infusion chemotherapy combined with interferon. *Oncology* 2010;78(Suppl 1):142–7.
18. Diaz BV, Lenoir MC, Ladoux A, et al. Regulation of vascular endothelial growth factor expression in human keratinocytes by retinoids. *J Biol Chem* 2000;275:642–50.
19. Hosui A, Hennighausen L. Genomic dissection of the cytokine-controlled STAT5 signaling network in liver. *Physiol Genomics* 2008;34:135–43.
20. Hosui A, Kimura A, Yamaji D, et al. Loss of STAT5 causes liver fibrosis and cancer development through increased TGF-{beta} and STAT3 activation. *J Exp Med* 2009;206:819–31.
21. Cui Y, Hosui A, Sun R, et al. Loss of signal transducer and activator of transcription 5 leads to hepatosteatosis and impaired liver regeneration. *Hepatology* 2007;46:504–13.
22. Onitsuka A, Yamada N, Yasuda H, et al. Rapid growth of hepatocellular carcinoma after or during interferon treatment of chronic hepatitis C: report of three cases. *Surg Today* 1996;26:126–30.

J Gastroenterol (2012) 47:577–585
DOI 10.1007/s00535-011-0522-7

ORIGINAL ARTICLE—LIVER, PANCREAS, AND BILIARY TRACT

Long-term effect of lamivudine treatment on the incidence of hepatocellular carcinoma in patients with hepatitis B virus infection

Mika Kurokawa · Naoki Hiramatsu · Tsugiko Oze · Takayuki Yakushijin · Masanori Miyazaki · Atsushi Hosui · Takuya Miyagi · Yuichi Yoshida · Hisashi Ishida · Tomohide Tatsumi · Shinichi Kiso · Tatsuya Kanto · Akinori Kasahara · Sadaharu Iio · Yoshinori Doi · Akira Yamada · Masahide Oshita · Akira Kaneko · Kiyoshi Mochizuki · Hideki Hagiwara · Eiji Mita · Toshifumi Ito · Yoshiaki Inui · Kazuhiro Katayama · Harumasa Yoshihara · Yasuharu Imai · Eijirou Hayashi · Norio Hayashi · Tetsuo Takehara

Received: 30 August 2011 / Accepted: 29 November 2011 / Published online: 11 January 2012

Abstract
Background Nucleotide analogues have recently been approved for the treatment of patients with hepatitis B virus (HBV) infection. However, it is still controversial whether the decrease of HBV-DNA amount induced by treatment with nucleotide analogues can reduce the risk of hepatocellular carcinoma (HCC) development in HBV patients.

Methods A total of 293 HBV patients without HCC who were treated with lamivudine (LAM) were enrolled in a multicenter trial. The incidence of HCC was examined after the start of LAM therapy, and the risk factors for liver carcinogenesis were analyzed. The mean follow-up period was 67.6 ± 27.4 months.

Results On multivariate analysis for HCC development in all patients, age ≥50 years, platelet count $<14.0 \times 10^4/mm^3$, cirrhosis, and median HBV-DNA levels of ≥4.0 log copies/ml during LAM treatment were significant risk factors. The cumulative carcinogenesis rate at 5 years was

Electronic supplementary material The online version of this article (doi:10.1007/s00535-011-0522-7) contains supplementary material, which is available to authorized users.

M. Kurokawa · N. Hiramatsu (✉) · T. Oze · T. Yakushijin · M. Miyazaki · A. Hosui · T. Miyagi · Y. Yoshida · H. Ishida · T. Tatsumi · S. Kiso · T. Kanto · A. Kasahara · T. Takehara
Department of Gastroenterology and Hepatology, Osaka University Graduate School of Medicine 2-2, Yamadaoka, Suita, Osaka 565-0871, Japan
e-mail: hiramatsu@gh.med.osaka-u.ac.jp

S. Iio
Higashiosaka City General Hospital, Higashiosaka, Japan

Y. Doi
Otemae Hospital, Osaka, Japan

A. Yamada
Sumitomo Hospital, Osaka, Japan

M. Oshita
Osaka Police Hospital, Osaka, Japan

A. Kaneko
NTT West Osaka Hospital, Osaka, Japan

K. Mochizuki · H. Hagiwara · N. Hayashi
Kansai Rosai Hospital, Amagasaki, Japan

E. Mita
National Hospital Organization Osaka National Hospital, Osaka, Japan

T. Ito
Osaka Kouseinenkin Hospital, Osaka, Japan

Y. Inui
Hyogo Prefectural Nishinomiya Hospital, Nishinomiya, Japan

K. Katayama
Osaka Medical Center for Cancer and Cardiovascular Disease, Osaka, Japan

H. Yoshihara
Osaka Rousai Hospital, Sakai, Japan

Y. Imai
Ikeda Municipal Hospital, Ikeda, Japan

E. Hayashi
Kinki Central Hospital of Mutual Aid Association of Public School Teachers, Itami, Japan

3% in patients with chronic hepatitis and 30% in those with cirrhosis. For the chronic hepatitis patients, the log-rank test showed the significant risk factors related to HCC development to be age ≥50 years, platelet count $<14.0 \times 10^4/mm^3$, and hepatitis B e antigen negativity, but median HBV-DNA levels of <4.0 log copies/ml (maintained viral response, MVR) did not significantly suppress the development of HCC. In cirrhosis patients, however, the attainment of MVR during LAM treatment was revealed to reduce the risk of HCC development.

Conclusions These results suggest that the incidence of HCC in HBV patients with cirrhosis can be reduced in those with an MVR induced by consecutive LAM treatment.

Keywords Lamivudine · Chronic hepatitis B · Cirrhosis · Hepatocellular carcinoma · HBV-DNA level

Abbreviations

HBV	Hepatitis B virus
HCC	Hepatocellular carcinoma
LAM	Lamivudine
ADV	Adefovir
ETV	Entecavir
Hbs Ag	Hepatitis B surface antigen
PCR	Polymerase chain reaction
TMA	Transcription-mediated amplification
IVR	Initial viral response
MVR	Maintained viral response
HBe Ag	Hepatitis B e antigen
CT	Computed tomography
MRI	Magnetic resonance imaging
ALT	Alanine aminotransferase

Introduction

More than 350 million people worldwide suffer from chronic infection with hepatitis B virus (HBV) [1–3]. Chronic HBV infection eventually leads to the development of cirrhosis and hepatocellular carcinoma (HCC), and raises the risk of hepatic disease-related death [4–6]. In Japan, up to 15% of HCC patients are diagnosed with HBV-related liver disease [7].

HCC is one of the most common malignancies in Japan and its incidence has been increasing over the past 30 years. Recently, various treatments such as transcatheter arterial embolization/chemoembolization, radio-frequency ablation, and hepatic resection have been reported to yield significant improvements in overall patient survival [8–11]. However, HCC relapse has thus far been observed in a majority of treated patients due to its highly malignant potential. In this regard, successful treatment of chronic HBV infection should prevent the patient's liver from progressing to cirrhosis and reduce the risk of HCC development. In recent years, the treatment of chronic hepatitis has changed greatly with the development of various antiviral therapies with nucleoside/nucleotide analogues such lamivudine (LAM), adefovir (ADV), and entecavir (ETV) [12–15]. LAM has long been used against chronic hepatitis, and many reports have demonstrated that LAM is effective in stabilizing inflammatory activity, suppressing HBV-DNA replication, and improving liver histological findings in chronic hepatitis patients [16, 17] and in HBV-related cirrhosis patients [18]. Furthermore, LAM has been reported to reduce the incidence of HCC in patients with chronic hepatitis B [19]. However, it is still controversial whether or not treatment using nucleotide analogues can reduce the risk of HCC development in HBV-infected patients [20, 21], and the relationship between the effect of HBV suppression and HCC development during LAM treatment has not yet been discussed in detail. Also, the risk factors for HCC development in HBV-infected patients who have been treated with LAM have not been sufficiently evaluated. In this study, we aimed to clarify whether the decrease of HBV-DNA amount induced by LAM therapy could reduce the incidence of HCC in HBV-infected patients.

Patients and methods

Patient selection and study design

This study was conducted at Osaka University Hospital and other institutions participating in the Osaka Liver Forum in Japan. The subjects were 293 consecutive patients with HBV infection who underwent continuous LAM therapy for more than 24 weeks from September 2000 to September 2006. All patients tested positive for hepatitis B surface antigen (HBs Ag) or had detectable levels of HBV DNA in their sera according to findings from a polymerase chain reaction (PCR)-based method or a transcription-mediated amplification (TMA) method. Exclusion criteria were patients with anti-hepatitis C antibody, anti-human immunodeficiency virus antibody, and other liver diseases (alcoholic liver disease, drug-induced liver disease, and autoimmune hepatitis). Also excluded were patients with a history of HCC and those who developed HCC within the first 24 weeks of the follow-up period after the initiation of LAM therapy (because of the possibility that microscopic HCC had been present before the initiation of treatment).

All patients were treated with 100 mg of LAM daily. Of the 293 patients, 129 underwent ADV (10 mg/day) therapy in addition to receiving ongoing LAM treatment. For 43 patients who started ETV administration in lieu of LAM, the observation period was terminated when they started

ETV. LAM resistance was confirmed by virological breakthrough and was defined as an increase in serum HBV-DNA by >1 $\log_{10}$ greater than the nadir [22]. If virological breakthrough developed and alanine aminotransferase (ALT) was elevated over the upper normal limit, the patients received add-on ADV at 10 mg/day.

In this study, all patients were examined for serum HBV-DNA level just before therapy initiation and every 6 months during treatment. The initial viral response (IVR) was defined as HBV-DNA <4.0 log copies/ml in the first 24 weeks of the follow-up period after the initiation of LAM therapy, and the maintained viral response (MVR) was defined as median HBV-DNA levels of less than 4.0 log copies/ml measured every 6 months during therapy.

This study protocol followed the ethical guidelines of the Declaration of Helsinki amended in 2008, and informed consent was obtained from each patient.

HBV testing

HBs Ag, hepatitis B e antigen (HBe Ag) and anti-hepatitis B e antibody (anti-HBe) levels were examined by chemiluminescence immunoassay or enzyme immunoassay. HBV DNA was measured by a PCR-based method (Amplicor HBV monitor; Roche Diagnostics, Tokyo, Japan) or a TMA method (TMA-HPA; Fujirebio, Tokyo, Japan), which have lower detection limits of 2.6 and 3.7 log copies/ml, respectively. The LAM-resistant YMDD mutant virus was examined by a PCR-ELMA method. Serum samples were stored frozen at −80°C.

Diagnosis of HCC and cirrhosis

Ultrasonography was carried out before LAM therapy and every 3–6 months during the follow-up period. New space-occupying lesions detected or suspected at the time of ultrasonography were further examined by computed tomography (CT), magnetic resonance imaging (MRI), or hepatic angiography. HCC was diagnosed by the presence of typical hypervascular characteristics on angiography, in addition to the findings from CT or MRI. If no typical image of HCC was observed, fine-needle aspiration biopsy was carried out with the patient's consent or the patient was carefully followed until a diagnosis was possible with definite observation by CT, MRI, or hepatic angiography. Cirrhosis was diagnosed by liver biopsy or laparoscopy, and for patients without this information, by clinical data, imaging modalities, and portal hypertension.

Statistical analysis

Quantitative variables were expressed as means ± SD. Quantitative variables at the baseline were compared among two groups, the chronic hepatitis and cirrhosis groups, using the Mann–Whitney *U*-test. Categorical data, such as gender and status of HBe Ag, were compared using Fisher's exact test. The cumulative incidence of HCC was evaluated with a Kaplan–Meiercurve and the differences between groups were analyzed by the log-rank test. For multivariate analysis to investigate factors affecting the cumulative incidence of HCC, Cox's regression analysis was carried out. A value of $p < 0.05$ (two-tailed) was considered to be statistically significant. All calculations were performed with SPSS version 15.0J (SPSS, Chicago, IL, USA).

Results

Baseline characteristics of patients

The baseline clinical features of the enrolled patients before LAM administration are shown in Table 1. The mean age of the patients was 48.0 ± 10.7 years, 214 (73%) of the entire group were male, and 163 (56%) tested positive for HBe Ag. Of the 293 patients, 205 (70%) were diagnosed as having chronic hepatitis and 88 (30%) as having cirrhosis. The median HBV-DNA level was 7.0 (range 3.0 to 8.5<) log copies/ml. At baseline, the aspartate aminotransferase (AST) level was 131 ± 151 IU/l, the ALT level was 203 ± 252 IU/l, the total bilirubin level was 1.2 ± 1.6 mg/dl, the albumin (Alb) level was 3.8 ± 0.5 g/dl, and the platelet count was 13.7 ± 5.4 × 10^4/mm^3. The mean follow-up period for all patients was 67.6 ± 27.4 months, with a range of 12–110 months from the start of LAM treatment. There were significant differences between patients with chronic hepatitis and those with liver cirrhosis in age, AST, ALT, total bilirubin, Alb, and platelet counts.

Cumulative incidence of development of HCC

Figure 1a shows the Kaplan–Meier curve of the cumulative HCC incidence for all HBV patients treated with LAM or LAM plus ADV. Of the 293 patients with HBV infection, 32 (10.9%) developed HCC and the cumulative carcinogenesis rate was 6% at 3 years, 12% at 5 years, and 15% at 7 years.

Figure 1b shows the Kaplan–Meier curve of the cumulative HCC incidence according to initial diagnosis (chronic hepatitis vs. cirrhosis). Eight (4%) of the 205 enrolled chronic hepatitis patients developed HCC and the cumulative carcinogenesis rate was 2% at 3 years, 3% at 5 years, and 5% at 7 years. On the other hand, 24 (27%) of the 88 enrolled cirrhosis patients developed HCC and the cumulative carcinogenesis rate was 15% at 3 years, 30% at 5 years, and 35% at 7 years.

Table 1 Patient characteristics

Factor	All	Chronic hepatitis	Cirrhosis	*p* value
Number of patients	293	205	88	
Age (years)	48.0 ± 10.7	46.3 ± 10.7	51.9 ± 9.8	<0.001**
Sex (male/female)	214/79	147/58	67/21	0.475
HBe Ag (positive	163 (56%)	121 (59%)	42 (48%)	0.068
HBV DNA (log copies/ml)[a]	7.0 (3.0 to 8.5<)	6.8±1.1	6.6 ± 1.1	0.162
AST (IU/l)	131 ± 151	143 ± 162	104 ± 120	0.045*
ALT (IU/l)	203 ± 252	235 ± 269	129 ± 189	<0.001**
Total bilirubin (mg/dl)	1.2 ± 1.6	0.9 ± 0.6	1.8 ± 2.7	<0.001**
Alb (g/dl)	3.8 ± 0.5	3.9 ± 0.4	3.5 ± 0.6	<0.001**
Platelets ($\times 10^4$/mm^3)	13.7 ± 5.4	15.6 ± 9.3	9.3 ± 3.8	<0.001**
Follow-up period (months)	67.6 ± 27.4	68.5 ± 26.5	65.5 ± 29.5	0.393

HBe Ag Hepatitis B e antigen, *HBV* hepatitis B virus, *AST* aspartate aminotransferase, *ALT* alanine aminotransferase, *Alb* albumin

[a] Values are expressed as medians

* $p < 0.05$, ** $p < 0.001$, comparing patients with chronic hepatitis and those with liver cirrhosis using the Mann–Whitney *U*-test for quantitative variables and Fisher's exact test for categorical variables

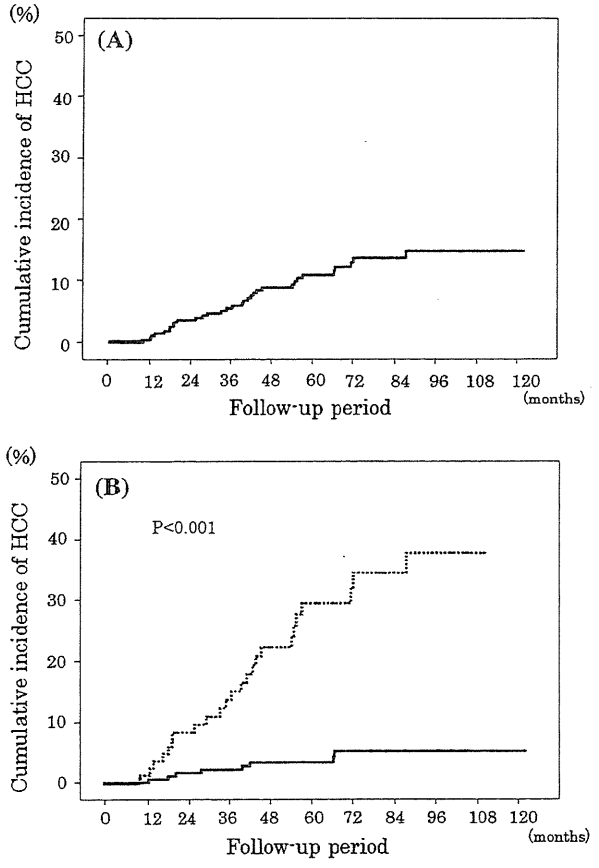

Fig. 1 Cumulative incidence of development of hepatocellular carcinoma (*HCC*) in patients with hepatitis B virus infection treated with lamivudine (LAM). **a** All cases; **b** chronic hepatitis or cirrhosis. *Solid line* Chronic hepatitis, *dotted line* cirrhosis

Risk factors for cumulative incidence of HCC development in all HBV-infected patients

Univariate analysis with the log-rank test was performed for all HBV-infected patients treated with LAM, with the results shown in Table 2. Univariate analysis with the log-rank test showed that the following were significant risk factors for the development of HCC: older age (≥50 years) ($p < 0.001$), cirrhosis ($p < 0.001$), high total bilirubin level (>1.2 g/dl) ($p = 0.004$), low Alb level (<3.8 g/dl) ($p = 0.019$), low platelet count (<14 × 10^4/mm^3) ($p < 0.001$), and non-MVR ($p = 0.035$).

Stepwise multivariate analyses of four of these variables were performed by Cox's regression analysis for all patients treated with LAM with the results shown in Table 3. The analysis indicated the following factors as independent significant risk factors related to the development of HCC: age ≥50 years [hazard ratio (HR) 3.20, 95% confidence interval [CI] 1.08–9.53, $p = 0.036$], platelet count <14.0 × 10^4/mm^3 (HR 4.76, 95% CI 0.05–0.96, $p = 0.045$), cirrhosis (HR 4.64, 95% CI 1.75–12.4, $p = 0.002$), and non-MVR (HR 2.70, 95% CI 1.09–6.56, $p = 0.032$).

Cumulative incidence of and risk factors for HCC development in patients with chronic hepatitis and cirrhosis

The results of univariate analysis with the log-rank test for the development of HCC in chronic hepatitis patients treated with LAM are shown in Table 4, and the following were significant risk factors: older age (≥50 years) ($p = 0.002$), HBe Ag negativity ($p = 0.005$), and low platelet count (<14 × 10^4/mm^3) ($p = 0.004$). Suppression of median HBV-DNA levels to <4.0 log copies/ml by LAM treatment was not associated with the development of HCC in the chronic hepatitis patients. Only non-MVR (median HBV-DNA amount ≥4.0 log copies/ml) was shown to be a significant risk factor for the development of HCC in the cirrhosis patients ($p = 0.029$), while the factors of age, HBe Ag status, and platelet count were not significant in these patients (Table 4).